A MODEL TO INVESTIGATE THE INFLUENCE OF SUSPENDED SEDIMENT ON THE MASS TRANSPORT OF A POLLUTANT IN OPEN CHANNEL FLOW

by

Raymond Scott Chapman
B.S. May 1975, Old Dominion University

A Thesis Submitted to the Faculty of
Old Dominion University in Partial Fulfillment of the
Requirements for the Degree of

MASTER OF ENGINEERING

CIVIL ENGINEERING

OLD DOMINION UNIVERSITY
March, 1977

Approved by:

Chin Y. Kuo (Director)

ABSTRACT

A MODEL TO INVESTIGATE THE INFLUENCE
OF SUSPENDED SEDIMENT ON THE MASS TRANSPORT
OF A POLLUTANT IN OPEN CHANNEL FLOW

Raymond Scott Chapman
Old Dominion University, 1977
Director: Dr. Chin Y. Kuo

The environmental impact of the transport of pollutants in open channel flow has for many years been of interest due to the continuous introduction of heavy metals, pesticides, herbicides, and other foreign substances into natural waterways. In order to fully understand this transport process, it is necessary to examine the significance of its individual components. In the present study an explicit two-dimensional finite difference model, designed to investigate the influence of suspended sediment on the pollutant transport process, is presented. Specific attention is directed toward examining the role of suspended sediment in 1) the turbulent vertical transport mechanism in a stratified flow, and 2) pollutant uptake due to sorption. Results presented indicate that suspended sediment plays a major role in the pollutant transport process, and subsequently, any meaningful attempt to model the fate of a pollutant

in an alluvial channel must account for the presence of a suspended sediment concentration profile. Similarly, the vertical and longitudinal pollutant concentration distributions provided by the model may be utilized to improve upon the predictive capacities of existing water quality models.

ACKNOWLEDGEMENTS

My sincerest thanks go to the members of my committee, Dr. Chin Kuo, Dr. William Drewry, Dr. Chester Grosch, and Dr. Charles Whitlock (of NASA Langley Research Center), for their guidance and assistance throughout the course of this study. In addition, I would like to thank Dr. Earl Kindle of the Physics and Geophysical Sciences Department and Mr. John Cox, a fellow graduate student, for many helpful and enlightening discussions. To Miss Nancy Miller, for her accurate technical typing, and Mr. Henry Wong, for his excellent work in drafting figures, I extend my genuine appreciation. Finally, the fellowship which made this work possible was provided by a grant from NASA Langley Research Center to the Graduate Research Participation Program in Aeronautics at Old Dominion University.

TABLE OF CONTENTS

CHAPTER I

INTRODUCTION

The environmental impact of the transport of pollutants in open channel flow has for many years been of interest due to the continuous introduction of heavy metals, pesticides, herbicides, and other foreign substances into natural waterways. In order to fully understand this transport process it is necessary to examine the significance of its individual components. Since the initial investigations of Elder (1959), much research has been directed toward modeling the influence of various factors such as bottom sediment, "dead zones," and bedload on the pollutant transport mechanism.

Shih and Gloyna (1969) utilized a one-dimensional convective-dispersion model with a sorption function to examine the influence of bottom sediment on the mass transport of radionuclides in streams. Comparison of predicted results with observed data from flume experiments led to the conclusion that the effects of bottom sediment on the pollutant mass transport process could not be neglected in a model simulation.

A similar model was adopted by Thackston and Schnelle (1970) to predict the effects of "dead zones" (pockets of little or no flow along stream banks) on the pollutant

transport process. To examine the storage effects of "dead zones," methods for estimating values of volume and residence time parameters were investigated. Agreement between experimental and computed results suggest that the methods for predicting the effects of "dead zones" on longitudinal dispersion are valid.

Using a one-dimensional stochastic model developed by Yang and Sayre (1971), Shen and Cheong investigated the effects of bedload on the mass dispersion of a pollutant. Considering an instantaneous injection of contaminated sediment particles, they suggest:

> Contaminants such as herbicides, pesticides, radioisotopes can attach to sediment particles and move as bedload in a stream, and the transport and dispersion of contaminants such as radioactive waste, can be affected by the dispersion characteristics of the sediment particles.

Similar ideas have been suggested with respect to the influence of suspended sediment on the pollutant mass transport process. In an assessment of the transport of radionuclides by streams (Sayre et al., 1963), it is concluded that:

> Available evidence indicates that sorption of waste materials from solution by stream sediments is the rule rather than the exception. Experiments have demonstrated that sorption of radioactive components from dilute solutions may exceed 90 percent, and that the concentration of radioactivity on the surface of sediment particles may become many thousands of times as great as the concentration in the surrounding liquid.

Reporting on the presence of DDT and Dieldrin in rivers, Breindenberg and Lichtenberg (1963) concluded from results presented by Berck (1953) that:

> . . . chlorinated hydrocarbons are adsorbed on the suspended solids in rivers. Thus, the silts common to some rivers may effectively remove pesticides from water.

In an experimental investigation of sorption of pesticides by clay minerals, Huang and Liao (1970) reported that DDT, Dieldren and Heptachlor are readily sorbed by clay minerals from aqueous solutions. As the suspended solids settle out and accumulate as bottom sediment, high concentration of pollutant in the substrate may result. Subsequently, Huang and Liao suggest that:

> Under certain conditions, part of the sorbed pesticides can be desorbed and released into the water where they are maintained by a dynamic equilibrium system. Consequently, pesticidal desorption provides a continuous supply of toxic material to water and creates many serious water pollution problems.

Reimer and Krenkel (1974) in an experimental study of the uptake of Mercury by suspended sediment concluded that:

> Because inorganic mercury binds with sands, clays, and various organics, the contention that mercury pollution is transported in our waterways by sediment is supported. For example, the appearance of mercury contamination in Kentucky Lake, which is over 100 miles from mercury contaminated

Pickwick Lake, the only known source of mercury in the system, can be explained on this basis.

Thus, in an attempt to shed some light on this potential environmental hazard, an explicit two-dimensional finite difference model designed to investigate the influence of suspended sediment on the pollutant mass transport process is presented. Specific attention is directed toward examining the role of suspended sediment in 1) the turbulent vertical transport mechanism in a stratified flow, and 2) pollutant uptake due to sorption. The model developed in this study provides a quantitative description of vertical and longitudinal pollutant concentration distributions which may be utilized to improve upon the predictive capabilities of existing water quality models.

CHAPTER II

MODEL FORMULATION

Governing Differential Equation

Based on the principle of conservation of mass, the two-dimensional unsteady convective-diffusion equation for a neutrally buoyant, conservative pollutant is of the form (Pritchard 1971, Sayre 1968, Harleman 1967):

$$\frac{\partial C}{\partial t} + \frac{\partial (Cu)}{\partial x} + \frac{\partial (Cv)}{\partial y} = \frac{\partial}{\partial x}\left(e_x \frac{\partial C}{\partial x} \right) + \frac{\partial}{\partial y}\left(e_y \frac{\partial C}{\partial y} \right) + r \qquad (2.1)$$

where

$C = C(x,y,t)$ = concentration of pollutant,

$u = u(y)$ = time averaged velocity in the x direction,

$v = v(y)$ = time averaged velocity in the y direction,

$e_x = e_x(y)$ = longitudinal diffusion coefficient,

$e_y = e_y(y)$ = vertical diffusion coefficient, and

r = sorption function.

Assuming

1) steady, uniform, incompressible flow, and

2) $v(y) = 0$,

equation (2.1) becomes

$$\frac{\partial C}{\partial t} + u(y)\frac{\partial C}{\partial x} = e_x(y)\frac{\partial^2 C}{\partial x^2}$$

$$+ \frac{\partial}{\partial y}\left(e_y(y)\frac{\partial C}{\partial y} \right) + r \ . \qquad (2.2)$$

The coordinate system for equation (2.2) is oriented such that x defines the longitudinal direction along the centerline of the channel with positive x downstream. The positive y direction is defined vertically upward with y=0 corresponding to the channel bottom, and t representing time. Defining the following dimensionless parameters:

$$X = \frac{x}{D}$$

$$Y = \frac{y}{D}$$

$$U = \frac{u(y)}{U_*}$$

$$E_x = \frac{e_x(y)}{DU_*} \qquad (2.3)$$

$$E_y = \frac{e_y(y)}{DU_*}$$

$$T = \frac{tU_*}{D} \ .$$

where

D = depth of flow,

U_* = shear velocity = $\sqrt{\tau_o/\rho} = \sqrt{gRS_o} = \sqrt{gDS_o}$

g = acceleration of gravity,

$S_o = S_e$ = slope of the channel bottom = $\left(\frac{nV}{1.49\ R^{2/3}}\right)^2$

τ_o = boundary shear stress,

ρ = density of the fluid,

R = hydraulic radius of the channel,

n = Manning's roughness coefficient, and

V = mean velocity over the depth of flow,

equation (2.2) is written in the dimensionless form:

$$\frac{\partial C}{\partial T} + U\frac{\partial C}{\partial X} = E_X\frac{\partial^2 C}{\partial X^2} + \frac{\partial}{\partial Y}\left(E_Y\frac{\partial C}{\partial Y}\right) + r^* \qquad (2.4)$$

where r^* is a dimensionless sorption function.

Velocity Profile

The classical representation of the velocity profile in a turbulent shear flow is the von Karman-Prandtl logarithmic velocity distribution law (Vanoni 1941). When expressed in terms of the mean velocity over the depth of flow, the velocity law is written as

$$u(y) = V + \frac{U_*}{\kappa}\left(\ln\left(\frac{Y}{D}\right) + 1\right) \qquad (2.5)$$

where

κ = von Karman's constant.

In nondimensional form, equation (2.5) becomes

$$U = \frac{V}{U_*} + \frac{1}{\kappa}(\ln Y + 1) \quad . \qquad (2.6)$$

Realizing that equation (2.6) is undefined at Y=0, the velocity at the channel bottom is prescribed to be zero in accordance with a "no slip" condition. Subsequently, the velocity profile calculation starts at Y=.1.

Graf (1971) suggests that in the presence of suspended sediment, von Karman's constant κ tends to decrease with increasing concentration, with a subsequent increase in the magnitude of the velocity profile. It is fully recognized that alternative velocity relationships have been proposed to account for the presence of suspended sediment; however, the von Karman-Prandtl velocity law κ=.4 is adopted due to its theoretical applicability in investigating the turbulent diffusion coefficients.

Vertical Diffusion Coefficient

Considering a neutrally buoyant pollutant, the

exchange coefficient for momentum is defined as

$$e_m = \frac{\tau}{\rho \frac{\partial u}{\partial y}} \quad . \tag{2.7}$$

where

τ = shear stress.

Assuming a linear variation in the shear stress with depth and noting that $U_*^2 = \tau_o/\rho$, equation (2.7) becomes

$$e_m = \frac{U_*^2 \left(1 - \frac{y}{D}\right)}{\frac{\partial u}{\partial y}} \quad . \tag{2.8}$$

Differentiating equation (2.5) with respect to y, the vertical velocity gradient is expressed as

$$\frac{\partial u}{\partial y} = \frac{U_*}{\kappa y} \quad . \tag{2.9}$$

Subsequently, substitution of equation (2.9) into equation (2.8) yields

$$e_m = \kappa U_* y \left(1 - \frac{y}{D}\right) \quad . \tag{2.10}$$

In nondimensional form, equation (2.10) is written as

$$E_m = \kappa Y (1 - Y) \tag{2.11}$$

where

$$E_m = \frac{e_m}{DU_*} \tag{2.12}$$

In applying equation (2.11) to represent vertical diffusion in the present model, the effects of density stratification due to the presence of a suspended sediment concentration profile must be taken into account. Leendertse (1975) suggests that:

> In fluids with vertically stable density gradients, each vertical motion of water mass has to work against buoyancy forces induced by the density gradient. If the available kinetic energy of turbulent motion is insufficient to overcome this stabilizing effect, turbulence is inhibited and suppressed. As a consequence, the process of vertical momentum exchange will be lower than under the neutral stability (vertically stable) condition.

To model the relationship between the vertical exchange coefficient for momentum and the vertical diffusion coefficient, numerous empirical equations have been proposed of the form:

$$e_y = e_m(1 + a\ Ri)^{-b} \tag{2.13}$$

where by definition, the Richardson's Number

$$Ri = \frac{-g\ \frac{\partial \rho}{\partial y}}{\rho \left(\frac{\partial u}{\partial y}\right)^2} \tag{2.14}$$

and a and b are constants greater than zero. From equations (2.13) and (2.14), it is clear that for a highly stratified flow in which there is a large density gradient, the Richardson's Number becomes large, and subsequently, the vertical diffusion process is suppressed. In the present study, the values of the constants a and b are chosen such that

$$\frac{e_y}{e_m} = (1 + 3.33\ Ri)^{-3/2} \qquad (2.15)$$

as reported by Munk and Anderson (1948). Combining equations (2.11) and (2.15), the vertical diffusion coefficient is evaluated by

$$E_y = \frac{\kappa Y(1 - Y)}{(1 + 3.33\ Ri)^{+3/2}} \qquad (2.16)$$

Similar treatments of the vertical diffusion process in a stratified fluid are discussed by Harleman and Ippen (1967) and Jirka et al. (1975). Although equation (2.16) defines a vertical diffusion coefficient of zero at the free surface (Y=1), experimental evidence (Jobson and Sayre 1970) suggests that in reality the value of the vertical diffusion coefficient at the free surface is greater than zero. Consequently, in the present study,

the value of the vertical diffusion coefficient at the free surface is prescribed to be one-half of the calculated vertical diffusion coefficient at Y=.9.

Longitudinal Diffusion Coefficient

Historically, investigations of longitudinal diffusion in open channel flow have been concerned with evaluating constant one-dimensional dispersion coefficients. The relationship

$$\frac{E}{RU_*} = \text{constant}, \tag{2.17}$$

where

E = longitudinal dispersion coefficient,

is considered to be significant in relating the longitudinal dispersion coefficient to the flow condition (Sayre 1968). However, Glover (1964) reports that experimental values of equation (2.17) vary from 5-24 in laboratory flume experiments and from 15-800 in canals and natural streams. This discrepancy suggests that dispersion coefficients evaluated in laboratory studies may not be representative of the dispersion process in natural streams. Tennekes and Lumley (1972) state that "turbulence is not a feature of the fluid but of fluid flow," which implies that a laboratory experiment may not

accurately predict dispersion without accurately modeling the turbulent characteristics of the flow.

In an attempt to formulate an applicable representation for longitudinal diffusion as a function of depth, an alternative is to adopt what is called the "Four-Thirds Law" as discussed by Harleman (1966), Sayre (1968), and Blair (1976). In general, the "Four-Thirds Law" is written

$$e_x = \alpha G^{1/3} L^{4/3} \tag{2.18}$$

where

α = constant,

G = energy dissipation rate per unit mass, and

L = characteristic eddy length.

Turner (1973) suggests that in a steady flow characterized by a logarithmic velocity profile, the energy dissipation rate, G, can be evaluated as a function of the depth by

$$G(y) = U_*^2 \frac{\partial u}{\partial y} \tag{2.19}$$

Substitution of equation (2.9) into equation (2.19) yields

$$G(y) = \frac{U_*^3}{\kappa y} \tag{2.20}$$

Presently, the constant α, and the characteristic eddy length L must be determined experimentally for a given flow condition. If, however, a time averaged value of L is assumed constant, a new constant α', is defined such that

$$\alpha' = \alpha L^{4/3} \tag{2.21}$$

Substitution of equations (2.20) and (2.21) into equation (2.18) yields

$$e_x(y) = \frac{\alpha' U_*}{(\kappa y)^{1/3}} \tag{2.22}$$

Thus, given that a prescribed value of $e_x(y)$ occurs at a specified depth, the constant α' is uniquely determined and a diffusion coefficient distribution is extrapolated over the depth of flow by means of equation (2.22). In the present study, the prescribed value of $e_x(y)$ is specified at middepth or, at $Y=.5$. However, if experimental values of α and L are known, equation (2.22) is applied directly. In nondimensional form, equation (2.22) is expressed as

$$E_x = \frac{\alpha'}{D^{4/3} (\kappa Y)^{1/3}} \tag{2.23}$$

Suspended Sediment Profile

The steady state one-dimensional vertical turbulent diffusion equation for suspended sediment is of the form (Shen 1970):

$$-V_T \frac{\partial Cs}{\partial y} = \frac{\partial}{\partial y}\left(D_y \frac{\partial Cs}{\partial y} \right) \tag{2.24}$$

where

V_T = average particle fall velocity,

Cs = suspended sediment concentration, and

D_y = vertical turbulent diffusion coefficient for suspended sediment.

Direct integration of equation (2.24) yields

$$-V_T Cs = D_y \frac{\partial Cs}{\partial y} \tag{2.25}$$

which states that for an equilibrium sediment concentration profile, the quantity of suspended sediment settling must be balanced by the turbulent diffusion upward in the direction of decreasing concentration. Expressing the vertical turbulent diffusion coefficient as a function of the momentum transfer coefficient (Jobson and Sayre 1970),

$$D_y = \beta \, e_m \tag{2.26}$$

where the constant of proportionality β, is generally considered to be less than or equal to one. Graf (1971) concludes that for a fine particle size, β is equal to one, and for a coarse particle size β is less than one. However in the present model, β is assumed equal to one. Substitution of equation (2.10) into equation (2.25), with the subsequent integration yields,

$$Cs = Co\left(\frac{D - y}{y}\right)^{\frac{V_T}{\kappa U_*}} \tag{2.27}$$

where Co is a constant of integration. Defining Cs=Ca at a reference depth y=a where, in the present model, a/D=.1 equation (2.27) becomes

$$\frac{Cs}{Ca} = \left[\frac{a}{DY}\left(\frac{1 - y}{1 - \frac{a}{D}}\right)\right]^{Z} \tag{2.28}$$

where

Ca = reference concentration, and

$$Z = \frac{V_T}{\kappa U_*} .$$

Noting that the suspended sediment concentration given by equation (2.28) is undefined at the channel bottom or Y=0, and zero at the free surface or Y=1, the following

boundary conditions are imposed (Kuo, 1976):

1) the suspended sediment concentration at the channel bottom (Y=0) is equal to the reference concentration Ca,

2) the suspended sediment concentration at the surface (Y=1) is linearly extrapolated such that for a mean particle size <.0001 cm the concentration is prescribed to be that of the adjacent lower layer, and for a mean particle size >.63 cm the concentration is set equal to zero.

Consequently, calculation of the suspended sediment concentration is carried out between Y=.1, and Y=.9.

Sorption Function

In studies of equilibrium sorption (Poinke and Chester 1972, Huang and Liao 1970, Reimer and Krenkel 1974, Boucher and Lee 1972), the empirically derived Fruendlich equation is found to be representative of experimental results. As applied to the sorption of pollutants onto suspended sediment, the Fruendlich equation is written

$$\frac{W}{M} = kC^{1/m} \qquad (2.29)$$

where

W = weight of sorbed pollutant by M grams of suspended sediment,

C = concentration of pollutant in equilibrium with the suspended sediment, and

k,m = experimentally determined constants.

Solving equation (2.29) for the weight of sorbed pollutant and multiplying both sides by the suspended sediment concentration, yields

$$Ce = k\ Cs\ C^{1/m} \tag{2.30}$$

where

Ce = equilibrium concentration of sorbed pollutant.

Denoting r to be the time rate of change of sorbed pollutant,

$$-r = \frac{\partial Cas}{\partial t} = -k_s(Cas - Ce) \tag{2.31}$$

where

Cas = an average concentration of sorbed pollutant, and

k_s = mass transfer coefficient.

Therefore, substitution of equation (2.30) into equation (2.31) yields

$$-r = \frac{\partial Cas}{\partial t} = k_s(kCs\ C^{1/m} - Cas) \tag{2.32}$$

which when nondimensionalized becomes

$$-r^* = \frac{\partial Cas}{\partial T} = K_s(kCs\ C^{1/m} - Cas) \tag{2.33}$$

where

$$K_s = \frac{k_s D}{U_*} \tag{2.34}$$

Model Summary

In summary, the equations which make up the present model are as follows:

$$\frac{\partial C}{\partial T} + U\frac{\partial C}{\partial X} = E_x\frac{\partial^2 C}{\partial X^2} + \frac{\partial}{\partial Y}\left(E_y\frac{\partial C}{\partial Y}\right) + r^*$$

where

$$r^* = -\frac{\partial Cas}{\partial T} = -K_s(kCsC^{1/m} - Cas)$$

$$U = \frac{V}{U_*} + \frac{1}{\kappa}(\ln Y + \perp)$$

$$E_x = \frac{\alpha'}{D^{4/3}(\kappa Y)^{1/3}} \tag{2.35}$$

$$E_Y = \frac{\kappa Y(1 - Y)}{(1 + 3.33\ Ri)^{3/2}}$$

$$\frac{Cs}{Ca} = \left[\frac{a}{DY}\left(\frac{1 - Y}{1 - \frac{a}{D}}\right)\right]^Z$$

Implicit solution of the two unknowns C, the ambient concentration of pollutant, and Cas, the sorbed concentration of pollutant requires the reduction of large systems of nonlinear equations; subsequently, in the present model equations (2.4) and (2.33) are uncoupled by solving for Cas with C evaluated at the previous time step. Thus, the pollutant concentration field is explicitly computed subject to the following boundary and initial conditions:

1) The ambient and sorbed pollutant concentration fields are initially set equal to zero, or

$$C(X,Y,0) = 0, \text{ and} \qquad X > 0$$
$$Cas(X,Y,0) = 0.$$

2) A line source of strength C_1 is prescribed over the entire depth of flow at X=0, or

$$C(0,Y,T) = C_1. \qquad T \geq 0$$

3) Mass transfer across the free surface is specified to be zero, or

$$E_Y \frac{\partial C}{\partial Y} = 0. \qquad Y = 1$$

4) To simplify treatment of the effects of bottom sediment and bedload, a flux is prescribed to the channel bottom. Specifically, the pollutant concentration at the channel bottom is calculated as a linear function of the concentration gradient between Y=0 and Y=.1.

CHAPTER III

COMPUTATIONAL METHODS

Mass Transport Equation

To simplify programming procedures and minimize computation time, an explicit finite difference scheme is employed. The difference approximations are a modified upwind differencing method, where the derivatives are approximated forward in time, backward in the first derivative in space, and centered in the second derivatives in space. Therefore, the truncation error of this method is of order (Δx), (Δt), $(\Delta y)^2$. Overall the scheme is first order accurate, however, it possesses both the conservative and transportive properties. Roache (1972) in a discussion on the use of a first order accurate upwind method suggests that:

> . . . it is also possible to more accurately represent a derivative by using a nonconservative method, but the whole system is not more accurate if one's criteria for accuracy include the conservative property.

Realizing that conservation of mass must be maintained in a pollutant transport model, the conservative property is indeed an important criteria when assessing the accuracy of a numerical scheme. Defining that a finite difference method is transportive "if the effect of a pertubation

is advected in the direction of the velocity," Roache goes on to say,

> Innocuous and obvious as this definition may read, the fact is that the most frequently used methods do not possess this property. All methods which use center space derivatives for the advection term do not possess this property.

Furthermore Roache suggests that:

> The transportive property appears to be as fundamentally important, as physically significant as the conservative property. At least in the sense, upwind differencing schemes which possess the transportive property are more accurate than schemes with space-centered first derivatives.

Thus, although mathematically first order accurate, upwind differencing schemes may be preferable in pollutant transport modeling. However, Roache also points out that by adopting a non-centered difference operator to approximate the advection term, an artificial or numerical diffusion coefficient is introduced of the form:

$$ae(y) = \tfrac{1}{2}U\Delta X(1 - c) \qquad (3.1)$$

where

ae = numerical diffusion coefficient,

c = courant number = $\frac{U\ \Delta T}{\Delta X}$

ΔX = longitudinal space increment, and

ΔT = time increment.

Therefore, to account for the effects of the numerical diffusion coefficient, the value of ae is computed and subsequently subtracted from the longitudinal diffusion coefficient at every iteration. To verify this correction method, the linear one-dimensional convective-diffusion equation,

$$\frac{\partial C}{\partial t} + V\frac{\partial C}{\partial x} = E\frac{\partial^2 C}{\partial x^2} \qquad (3.2)$$

was solved numerically and compared to a known analytic solution subject to the following boundary and initial conditions:

$$C(0,t) = C_1 \qquad t \geq 0$$

$$C(x,0) = 0 \qquad x > 0$$

$$C(\infty,t) = 0 \qquad t \geq 0$$

Dailey and Harleman (1966) present an analytic solution to equation (3.2) which is of the form:

$$\frac{C}{Ci} = \tfrac{1}{2}\exp\left(\frac{Vx}{E}\right) \operatorname{erfc}\left(\frac{x + Vt}{2\sqrt{Et}}\right) + \tfrac{1}{2} \operatorname{erfc}\left(\frac{x - Vt}{2\sqrt{Et}}\right) \qquad (3.4)$$

where the complimentary error function, erfc(s)=1-erf(s) and the error function is defined as

$$\operatorname{erf}(s) = \frac{2}{\sqrt{\pi}} \int_0^s e^{-\xi^2}\, d\xi \qquad (3.5)$$

In evaluating the analytic solution presented in equation (3.4), the error function is approximated by means of the following series (Abramowitz and Stegun 1964):

$$\operatorname{erf}(s) = 1 - (a_1 q + a_2 q^2 + a_3 q^3 + a_4 q^4 + a_5 q^5)\exp(-s^2) \qquad (3.6)$$

where

$a_1 = .254829592$

$a_2 = -.284496736$

$a_3 = 1.421413741$

$a_4 = -1.453152027$

$a_5 = 1.061405429$

$p = .3275911$, and

$q = 1/(1 + ps)$

Figure (3.1) illustrates the close agreement between the numerical and analytic solution of equation (3.2).

Denoting the subscripts I,J,N, to represent the position of X, Y, and T, respectively, the finite difference approximations used in the present model are as follows:

$$\frac{\partial C}{\partial T} = \frac{1}{\Delta T}\left(C_{I,J,N+1} - C_{I,J,N}\right) \qquad (3.7)$$

$$U\frac{\partial C}{\partial X} = \frac{U_J}{\Delta X}\left(C_{I,J,N} - C_{I-1,J,N}\right) \tag{3.8}$$

$$E_x\frac{\partial^2 C}{\partial X^2} = \frac{(E_x - ae)_J}{(\Delta X)^2}\left(C_{I+1,J,N} - 2C_{I,J,N} + C_{I-1,J,N}\right) \tag{3.9}$$

$$\frac{\partial}{\partial Y}\left(E_Y\frac{\partial C}{\partial Y}\right) = \frac{1}{2(\Delta Y)^2}\left(E_{yJ+1} + E_{yJ}\right)\left(C_{I,J+1,N} - C_{I,J,N}\right) + \left(E_{yJ} + E_{yJ-1}\right)\left(C_{I,J,N} - C_{I,J-1,N}\right) \tag{3.10}$$

$$\frac{\partial Cas}{\partial T} = \frac{1}{\Delta T}\left(Cas_{I,J,N+1} - Cas_{I,J,N}\right) \tag{3.11}$$

In general, numerical stability is maintained provided that the time increment

$$\Delta T \leq \frac{1}{\frac{2(E_x - ae)}{(\Delta X)^2} + \frac{2E_Y}{(\Delta Y)^2} + \frac{U}{\Delta X}} \tag{3.12}$$

where maximum values of the turbulent diffusion coefficients, artificial diffusion coefficient and longitudinal velocity are used.

Richardson's Number

Investigation of the effects of a suspended sediment concentration profile on the vertical diffusion mechanism requires that the Richardson's Number be evaluated at each depth considered. Noting that the specific weight $\gamma=\rho g$, equation (2.14) is written,

$$Ri = \frac{-g \frac{\partial \gamma}{\partial y}}{\gamma \left(\frac{\partial u}{\partial y}\right)^2} \tag{3.13}$$

Substitution of equation (2.9) into equation (3.13) yields

$$Ri = \frac{-g \frac{\partial \gamma}{\partial y}}{\gamma \left(\frac{U_*}{\kappa y}\right)^2} \tag{3.14}$$

Assuming that the volume of suspended sediment is negligible with respect to the volume water, the specific weight γ is approximated as a function of depth by

$$\gamma(y) = \frac{\gamma_w}{1 - Cs(y) \times 10^{-6}} \tag{3.15}$$

where

γ_w = specific weight of water.

Therefore, by adopting a second-order accurate difference approximation, the vertical density gradient is evaluated

by

$$\frac{\partial \gamma}{\partial y} = \frac{\gamma_{J+1} - \gamma_{J-1}}{2\Delta y} \tag{3.16}$$

Figure (3.2) is a plot of Richardson's Number versus depth illustrating the sensitivity of the computed density gradient to the differencing increment in the y direction. The change in the Richardson's Number with mesh refinement is primarily due to the specification of boundary conditions at the channel bottom and free surface. Nonetheless, close agreement is maintained between Y=.2, and Y=.8 which is essentially the region of interest in the present study.

CHAPTER IV

MODEL SIMULATION

Numerical simulation is approached in three phases, namely

1) Dispersion experiments

2) Stratification experiments, and

3) Sorption experiments.

In all the above simulations, the following model parameters are held constant:

D = 20 ft

V = .5 ft/sec

Δt = 5 sec

Δx = 50 ft

Δy = 2 ft

Figure (4.1) illustrates the extent of the model simulation where

n = Manning's roughness coefficient,

Emag = value of the longitudinal diffusion coefficient prescribed at middepth, and

ds = mean particle size.

The first phase of simulation examines the response of the pollutant transport process to variations in flow condition without imposing a suspended sediment concentration profile. The flow condition is prescribed by

choice of a channel roughness as defined by Manning's roughness coefficient, and the magnitude of the longitudinal diffusion coefficient specified at middepth. Noting figure (4.1), Manning's roughness coefficients of .01, .03, and .06 are adopted as typical values for natural streams (Chow 1959), with a range for the longitudinal diffusion coefficient of 10, 50, and 100 ft^2/sec. In the present model, with the depth and mean velocity held constant, increases in the channel roughness results in increasing channel slopes, and subsequently greater shear velocities. Figure (4.2) is a nondimensional plot of velocity versus depth illustrating the increase in shear velocity with an increase in channel roughness. In addition, from equation (2.9) it is readily seen that with an increase in shear velocity, a subsequent increase in the velocity gradient occurs. A similar result is also indicated when plotting nondimensional longitudinal diffusion versus depth (Figure 4.3).

The second phase of experimentation examines the effect of stratification, due to the presence of a suspended sediment concentration profile, on the turbulent vertical mass transfer mechanism. Noting figure (4.1) the flow condition for this particular investigation is prescribed by choosing a typical Manning's

roughness coefficient of .03, and a magnitude of 50 ft^2/sec for the longitudinal diffusion coefficient. In order to vary the shape and magnitude of the suspended sediment concentration profile, reference suspended sediment concentrations of 100, 500, and 1000 ppm and mean particle sizes of .001, .005, and .01 mm are adopted. Figures (4.4) and (4.5) illustrate the change in the suspended sediment concentration profiles with varying reference suspended sediment concentrations and mean particle sizes. Thus, the variation in the suspended sediment concentration gradient, results in notable changes in the Richardson's Number distribution with depth (Figures (4.6) and (4.7)). Comparison of figures (4.4) and (4.6) reveals that the magnitude of the Richardson's Number is highly dependent on the suspended sediment concentration gradient; however, the distribution of the Richardson's Number over the depth of flow appears to be more sensitive to the magnitude of the velocity gradient. Similar results are indicated when comparing figures (4.5), and (4.7); however, for ds=.01 mm the decrease in suspended sediment concentration is so rapid that as the velocity gradient approaches zero no apparent increase in the Richardson's Number occurs. Recalling equation (2.16), the greater the Richardson's Number

the more significant the reduction in the turbulent vertical diffusion coefficient. This result becomes obvious when figures (4.6) and (4.7) are compared with figures (4.8) and (4.9), respectively.

The third phase of experimentation investigates the uptake of pollutant by suspended sediment due to sorption. The flow condition is the same as in phase 2, and in addition, the analysis is further restricted by selecting a typical reference suspended sediment concentration of 500 ppm, and a mean particle size of .005 mm (Figure 4.1). The sorption function presented in Chapter II is expressed as a first order reaction in terms of an equilibrium uptake of pollutant for a given suspended sediment concentration. Experimental results relating the equilibrium uptake of pollutant to suspended sediment concentration are well documented in the literature from which the Freundlich constants of the pollutants considered in the present model are obtained (Table 4.1). Sorption rates are expressed as rate constants derived by simply taking the reciprocal of an average time in seconds for equilibrium uptake of a given pollutant by clays, and or sand. To account for the heterogeneous composition of suspended sediment, the rate constants are treated parametrically and varied over three orders of magnitude.

TABLE 4.1

Approximate Freundlich Constants

Pollutant	k	1/m	Reference
Mercury	5×10^{-4}	1	Riemer & Krenkel (1974)
DDT	3×10^{-3}	3	Huang & Liao (1970)
Heptachlor	5×10^{-6}	5	Huang & Liao (1970)

CHAPTER V

RESULTS AND DISCUSSION

Results of the first phase of experimentation indicate that the model simulation is sensitive to the choice of both the channel roughness and the magnitude of the longitudinal diffusion coefficient. Figure (5.1) is a normalized plot of the pollutant concentration versus depth illustrating the influence of varying channel roughness on the vertical concentration profile. The increase in magnitude of the vertical concentration gradient with channel roughness is a direct result of the increase in the velocity gradient due to greater shear velocities. Normalized plots of the pollutant concentration versus longitudinal distance, figures (5,2a,b,c), are presented to illustrate the effect of an increase in magnitude of the longitudinal diffusion coefficient on the longitudinal distribution of pollutant. Two important features of the dispersion simulation are displayed in these figures. The first is that early in the simulation, or at t=200 sec, longitudinal diffusion initially dominates the dispersion process as indicated by the increase in magnitude of the concentration wave front with greater values of Emag. However,

as the simulation proceeds in time, the longitudinal concentration gradient decreases and advection dominates longitudinal diffusion as the system approaches steady state (Figures (5.2b,c)).

Results of the second phase of investigation reveal that damping of turbulent vertical mixing due to stratification caused by presence of a suspended sediment concentration profile, is a prominent feature of the pollutant transport process. Figure (5.3), a normalized plot of pollutant concentration versus depth, exhibits a pronounced vertical concentration gradient due to the lack of vertical mixing. Although the influence of a suspended sediment concentration profile is notable, figures (5.4a,b) illustrate the lack of significance of the variations in magnitude of the suspended sediment concentration and mean particle size on the degree of reduction of turbulent vertical diffusion coefficient corrected for the influence of stratification is less than 30% of the maximum momentum exchange coefficient, figures (4.8) and (4.9), it is apparent that irrespective of the magnitude of the suspended sediment concentration or mean particle sizes considered the damping of the vertical turbulent mixing mechanism is significant.

Analysis of the sorption experiments indicate that the uptake of Mercury, DDT, and Heptachlor by suspended

sediment must be considered a significant factor in the pollutant mass transport process. Mercury, the only inorganic compound investigated is affected least by the sorption mechanism; however, the uptake of mercury by suspended sediment is quite notable. Figure (5.5) illustrates the decrease in the magnitude of the vertical concentration profile with increases in the order of magnitude of the sorption rate parameter k_s. Furthermore, an important trend is seen in the decrease of pollutant concentration with depth due to increasing suspended sediment concentration. This feature is further illustrated in figures (5.6a,b), where normalized plots of concentration versus longitudinal distance are shown at Y=.2 and .5, respectively. These results suggest that the distribution of the suspended sediment concentration profile must be accurately represented when modeling the uptake of a pollutant by suspended sediment in natural streams. DDT and Heptachlor are organic pesticides which, by their chemical nature, are highly receptive to uptake due to sorption by suspended sediment. Figures (5.7) and (5.8) are normalized plots of concentration versus depth and longitudinal distance, respectively, illustrating the increase in uptake of DDT with increases in the order of magnitude

of the sorption parameter k_s. Similar results exhibited in figures (5.9) and (5.10) for Heptachlor suggest that the uptake of organic pesticides by suspended sediment is indeed significant.

CHAPTER VI

SUMMARY AND CONCLUSIONS

In summary, a two-dimensional convective-diffusion model has been applied successfully to investigate the effects of suspended sediment on the mass transport of pollutants in open channel flow. The analysis is restricted to examining the transport of a conservative, neutrally buoyant pollutant in a uniform turbulent shear flow. The numerical simulations performed lead to the following conclusions:

A. Application of mathematical models to investigate the pollutant transport process in natural streams requires the judicious choice of channel roughness, and a reasonable representation of longitudinal diffusion.

B. The suppression of the turbulent vertical mixing process, as a result of vertical density stratification due to the presence of a suspended sediment profile is shown to be significant.

C. The reduction of pollutant concentration due to uptake by suspended sediment suggests that the sorption mechanism is an important component of the mass transport process.

The present study has clearly illustrated the significance of a suspended sediment concentration profile on the pollutant mass transport process. In order to refine the results presented herein, further research is needed to improve upon the following:

A. As discussed in Chapter II, a von Karman's constant $\kappa=.4$ is adopted without correction for the presence of suspended sediment. However, if the suspended sediment size distribution is known, correction can be made by adjusting von Karman's constant according to the empirical relation presented by Einstein and Adbel-Aal (1972).

B. A theoretical approach to extrapolate a longitudinal diffusion coefficient profile has been proposed; however, experiment evidence is needed to test the applicability of the "Four-Thirds Law" to turbulent diffusion in natural streams.

C. Constant sorption rates are adopted in the present model, where in reality sorption rates are decreasing nonlinear functions. A possible means to more accurately represent sorption rates would be to develop an empirical rate function from experimental data.

D. In the present study, the analysis has been restricted to examining the fate of conservative pollutants. To account for the decay of a nonconservative pollutant

such as radionuclides, it is only necessary to subtract the concentration of pollutant computed by an experimental decay rate function from the values of C and Cas at every time iteration.

E. A constant longitudinal suspended sediment concentration at each depth is assumed throughout the present model. However, in applying the model to a physical situation, remote sensing techniques may be employed to provide a longitudinal distribution of surface suspended sediment concentrations with a minimal amount of field data for ground truth. Thus, by redefining the suspended sediment concentration reference level to be the free surface (a/D=1), vertical suspended sediment concentration distributions may be extrapolated as a function of the longitudinal variation of suspended sediment at the surface.

F. A prescribed flux is specified at the channel bottom to simplify modeling the sorption influence of bedload and bottom sediment. As previously mentioned, the effects of bedload and bottom sediment on the pollutant mass transport process have been investigated in two separate studies, hence, an interesting line of research would be to integrate the effects of bottom sediment, bedload, and suspended sediment into a single convective-diffusion model in an attempt to obtain a more detailed

understanding of the pollutant mass transport process.

REFERENCES

Abrahmowitz, M. and I.A. Stegun. Handbook of Mathematical Functions. National Bureau of Standards Applied Mathematics Series, No. 55, 1964.

Berck, B. "Microdetermination of DDT in Riverwater and Suspended Solids." Analytic Chemistry, Vol. 25, No. 8, p. 1253, August 1953.

Blair, C.H. "Similitude of Mass Transport in a Distorted Froude Model of an Estuary." A Ph.D Dissertation, School of Engineering, Old Dominion University, 1976.

Boucher, F.R. and G.F. Lee. "Adsorption of Lindane and Dieldren Pesticides on Unconsolidated Aquifer Sands." Environmental Science and Technology, Vol. 6, No. 6, pp. 538-543, 1972.

Breidenbach, A.W., and J.J. Lichtenberg. 'DDT and Dieldrin in Rivers: A Report of the National Water Quality Network." Science, Vol. 141, pp. 899-901, 1963.

Chow, V.T. Open Channel Hydraulics. New York: McGraw-Hill Book Co., 1959.

Dailey, J.W. and D.F.R. Harleman. Fluid Dynamics. Reading, Mass.: Addison Wesley Publishing Co., 1966.

Elder, J.W. "The Dispersion of a Marked Fluid in a Turbulent Shear Flow." Journal of Fluid Mechanics. Vol. 5 pp. 544-560, 1959.

Einstein, H.A. and F.M. Adbel-Aal. "Einstein Bedload Function for High Sediment Rates." Journal, Hydraulic Division, A.S.C.E., Vol. 98, No. HY 1, pp. 137-151, 1972.

Glover, R.E. "Dispersion of Dissolved and Suspended Materials in Streams." U.S.G.S. Prof. Paper, 433-b, 1964.

Graf, H.W. Hydraulics of Sediment Transport. New York: McGraw-Hill Book Co., 1971.

Gerald, C.F. Applied Numerical Analysis. Reading, Mass.: Addison Wesley Publishing Co., 1970.

Harleman, D.R.F. Estuary and Coastline Hydrodynamics. Ed. A.T. Ippen. New York: McGraw-Hill Book Co., 1966.

Harleman, D.F.R. and A.T. Ippen. "Two Dimensional Aspects of Salinity Intrusion in Estuaries: Analysis of Salinity and Velocity Distributions." Tech. Bulletin No. 13. Vicksburg, Miss.: Corps of Engineers, U.S. Army, 1967.

Huang, J. and C. Liao. "Adsorption of Pesticides by Clay Minerals." Journal, Sanitary Engineering Division, A.S.C.E., Vol. 96, No. SA 5, pp. 1057-1077, 1970.

Jirka, G.H. et al., "An Assessment of Techniques for Hydrothermal Prediction." Dept. of Civil Engineering, M.I.T., March 1976.

Jobson, H.E. and W.W. Sayre. "Vertical Transfer in Open Channel Flow." Journal, Hydraulic Division A.S.C.E., Vol. 96, No. HY 3, pp. 703-723, 1970.

Kuo, C.Y. "Sediment Routing in an In-Stream Settling Basin." In Proceedings of the National Symposium on Urban Hydrology, Hydraulics, and Sediment Control. University of Kentucky, Lexington, Kentucky, July 1976.

Leendertse, J.J. and S.K. Liu. "A Three Dimensional Model for Estuaries and Coastal Seas: Volume II, Aspect of Computation." Santa Monica, Calif.: The Rand Corp., R-1764-owrt, June 1976.

Munk, W.H. and E.R. Anderson. "Notes on a Theory of the Thermocline." Journal of Marine Research, No. 3, 1948.

Nordin, C.F. and R.S. McQuivey. "Suspended Load." Chapter 13 in River Mechanics. Ed. H.W. Shen, Water Resources Publications, 1972.

Poinke, H. and G. Chester. "Pesticide-Sediment-Water Interaction." Journal of Environmental Quality, Vol. 2, No. 1, p. 29, 1962.

Pritchard, D.W. "Two Dimensional Models," Chapter 2, In Estuarine Modeling, An Assessment. Ed. G.H. Ward and W.H. Espey, Jr., Austin, Texas: Tracor Inc., 1971.

Reimer, R.S. and P.A. Krenkel. "Kinetics of Mercury Adsorption and Desorption on Sediments." W.P.C.F., Vol. 46, No. 2, pp. 352-364, 1974.

Roache, P.J. Computational Fluid Dynamics. Alburquerque New Mexico: Hermosa Publishers, 1972.

Sayre, W.W. and F.M. Chang. "A Laboratory Investigation of Open Channel Dispersion Processes for Dissolved, Suspended and Floating Dispersants." U.S.G.S. Prof. Paper, 433-e, 1968.

Sayre, W.W., H.P. Guy, and A.R. Chamberlain. "Uptake and Transport of Radionuclides by Stream Sediment." U.S.G.S. Prof. Paper, 433-H, 1963.

Shen, H.W. and H.F. Cheong. "Dispersion of Contaminated Sediment Bedload." Journal, Hydraulic Division, A.S.C.E., Vol. 99, No. HY 11, pp. 1947-1965, 1973.

Shih, C. and E.F. Gloyna. "Influence of Sediments on the Transport of Solutes." Journal, Hydraulic Division, A.S.C.E., Vol. 95, No. HY 4, pp. 1347-1367, 1969.

Thackston, E.L. and K.B. Schnelle. "Predicting the Effects of Dead Zones on Stream Mixing." Journal, Sanitary Engineering Division, A.S.C.E., Vol. 96, No. SA 2, pp. 319-331, 1970.

Turner, J.S. Buoyancy Effects in Fluids. Cambridge, England: Cambridge University Press, 1973.

Vanoni, V.A. "Velocity Distribution in Open Channel Flow." Civil Engineering, Vol. 11, No. 6, pp. 356-357, June 1941.

Yang, C.T. and W.W. Sayre. "Stochastic Model of Sand Dispersion." Journal, Hydraulic Division, A.S.C.E., Vol. 97, No. HY 2, pp. 265-288, 1971.

LIST OF SYMBOLS

a = empirical constant equation (2.13)

ae = artificial diffusion coefficient

a_1 = constant equation (3.6)

a_2 = constant equation (3.6)

a_3 = constant equation (3.6)

a_4 = constant equation (3.6)

a_5 = constant equation (3.6)

b = empirical constant equation (2.13)

c = courant number

C = concentration of pollutant

C_1 = initial pollutant concentration

Cas = concentration of sorbed pollutant

Ce = equilibrium concentration of sorbed pollutant

Co = constant of integration

Cs = suspended sediment concentration

D = depth of flow

D_y = turbulent vertical diffusion coefficient for suspended sediment

ds = mean suspended sediment particle size

E = longitudinal dispersion coefficient

e_m = vertical momentum exchange coefficient

Emag = value of longitudinal diffusion coefficient prescribed at middepth

e_x = longitudinal diffusion coefficient

E_x = nondimension longitudinal diffusion coefficient

e_y = vertical diffusion coefficient

E_y = nondimensional vertical diffusion coefficient

g = acceleration of gravity

G = energy dissipation rate per unit mass of fluid

I = subscript denoting longitudinal cartesian direction

J = subscript denoting vertical cartesian direction

k = empirical Freundlich constant

k_s = sorption rate constant

K_s = nondimensional sorption rate constant

L = characteristic eddy length

m = empirical Freundlich constant

M = weight of suspended sediment

n = Manning's roughness coefficient

N = subscript denoting time

r = sorption function

r* = nondimensional sorption function

R = hydraulic radius of the channel

Ri = Richardson's Number

s = dummy argument equation (3.5)

$S_o=S_e$= slope of the channel

t = time

T = nondimensional time

u = longitudinal velocity component

U = nondimensional longitudinal velocity component

U_* = shear velocity

v = vertical velocity component

V = average longitudinal velocity

W = weight of sorbed pollutant

x = longitudinal cartesian direction

X = nondimensional longitudinal cartesian direction

y = vertical cartesian direction

Y = nondimensional vertical cartesian direction

V_T = average particle fall velocity

Z = exponent equation (2.28)

α = coefficient equation (2.18)

α' = coefficient equation (2.22)

β = coefficient equation (2.20)

γ = specific weight of water sediment mixture

γ_w = specific weight of water

Δt = time increment

Δx = longitudinal space increment

Δy = vertical space increment

κ = von Karman's constant

ξ = dummy variable of integration equation (3.5)

ρ = density of the fluid

τ = shear stress

τ_o = bottom shear stress

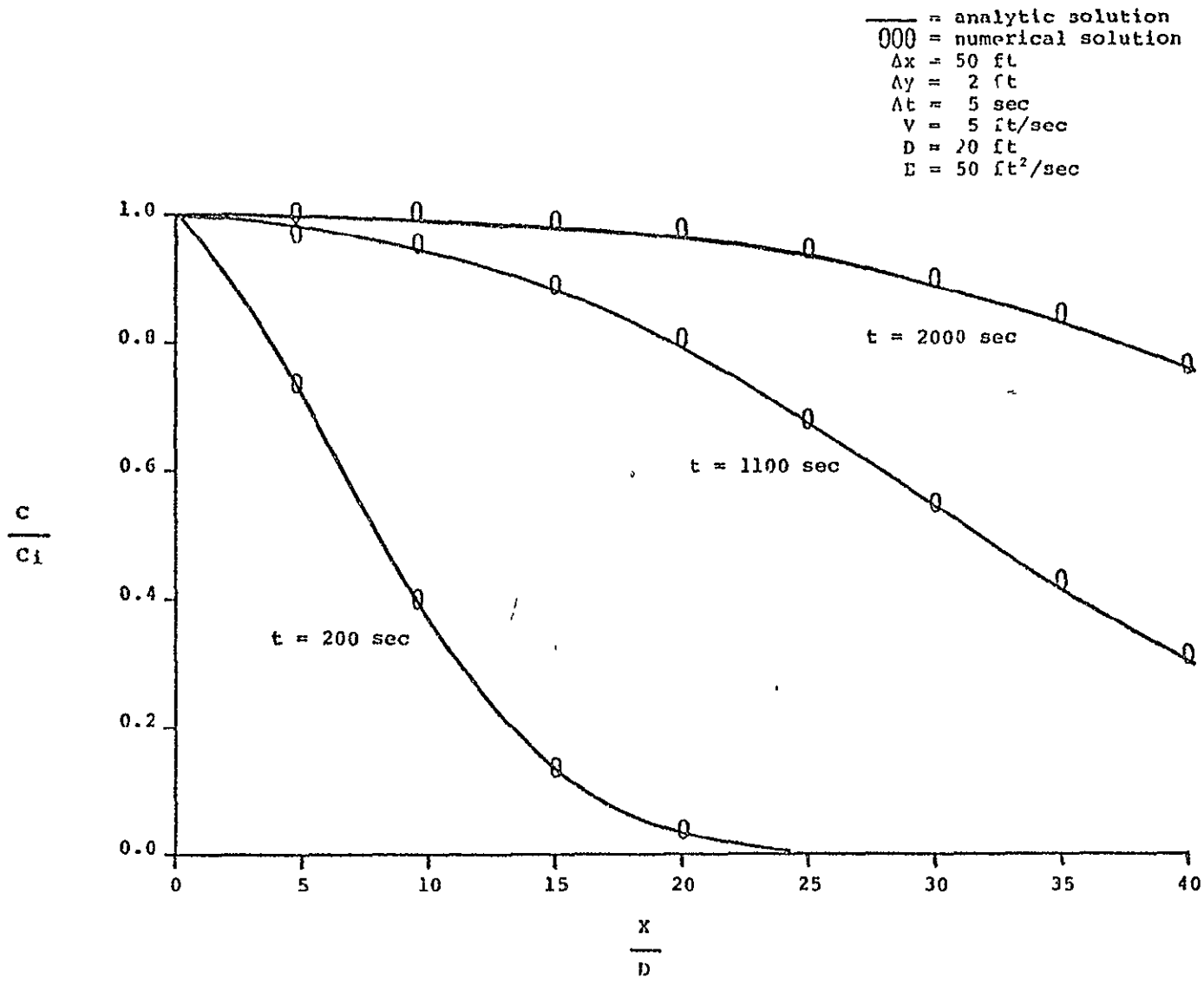

Figure 3.1 Comparison of analytic and numerical solutions.

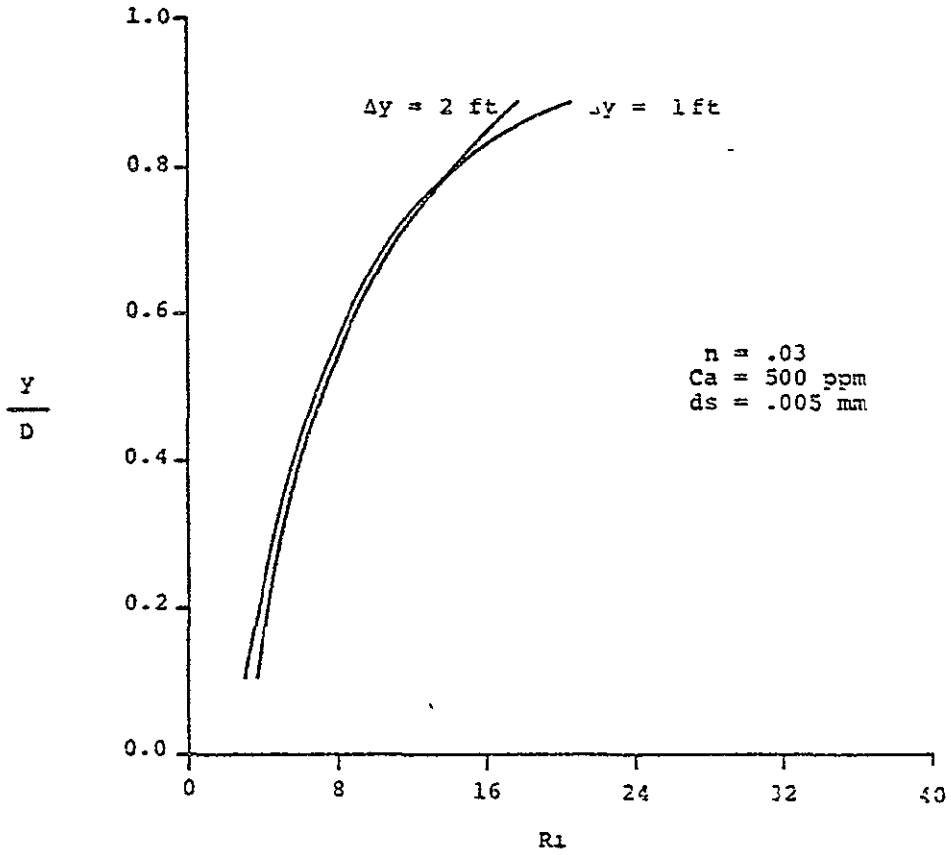

Figure 3 2 Vertical distribution of Richardson's number as a function of the vertical space increment Δy.

Dispersion Experiments

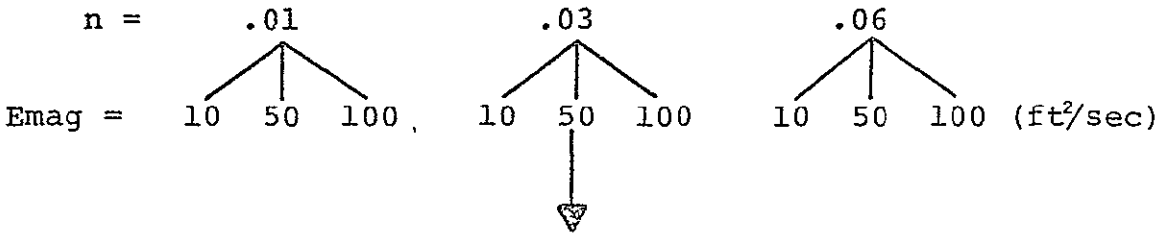

Stratification Experiments

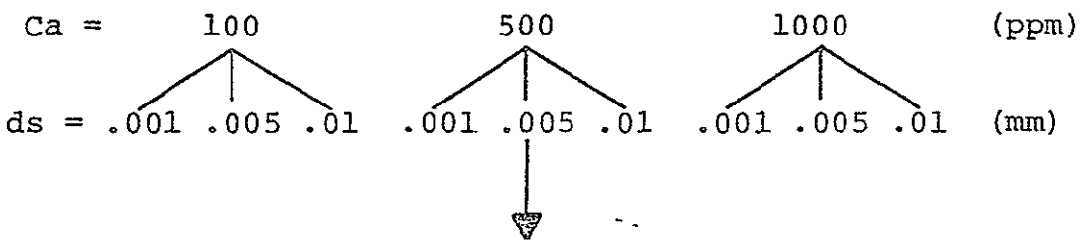

Sorption Experiments

	Mercury	DDT	Heptachlor	
	1×10^{-4}	1×10^{-5}	1×10^{-5}	
k_s =	5×10^{-4}	1×10^{-4}	1×10^{-4}	(1/sec)
	1×10^{-3}	1×10^{-3}	1×10^{-3}	

Figure 4.1 Model Simulations

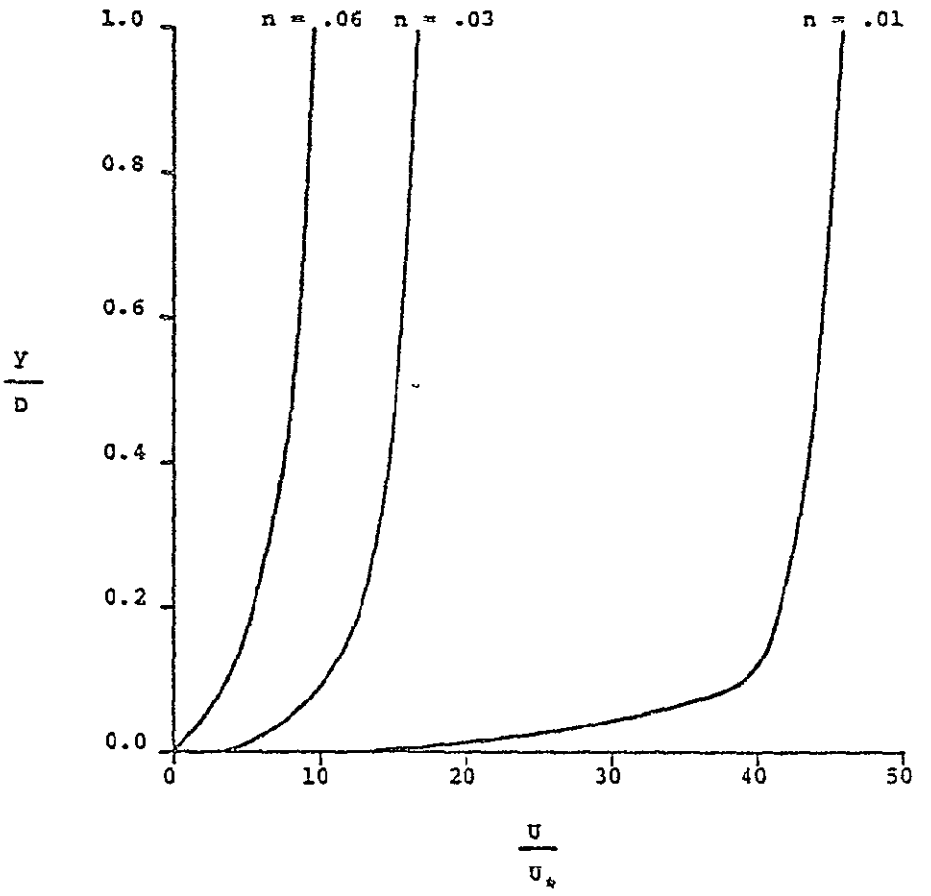

Figure 4.2 Vertical velocity distribution as a function of Manning's roughness coefficient n.

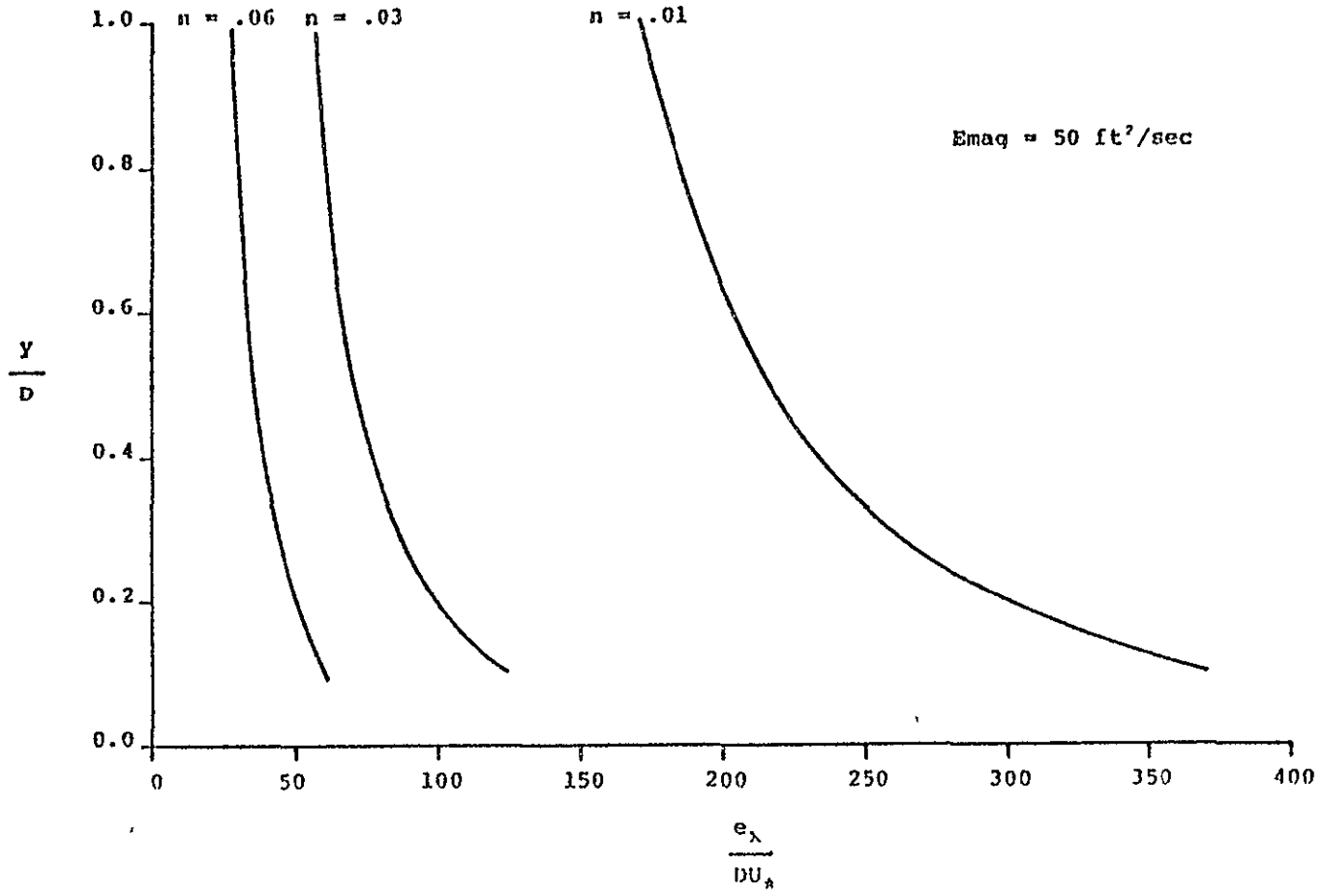

Figure 4.3 Vertical distribution of the longitudinal diffusion coefficient as a function of Manning's roughness coefficient n.

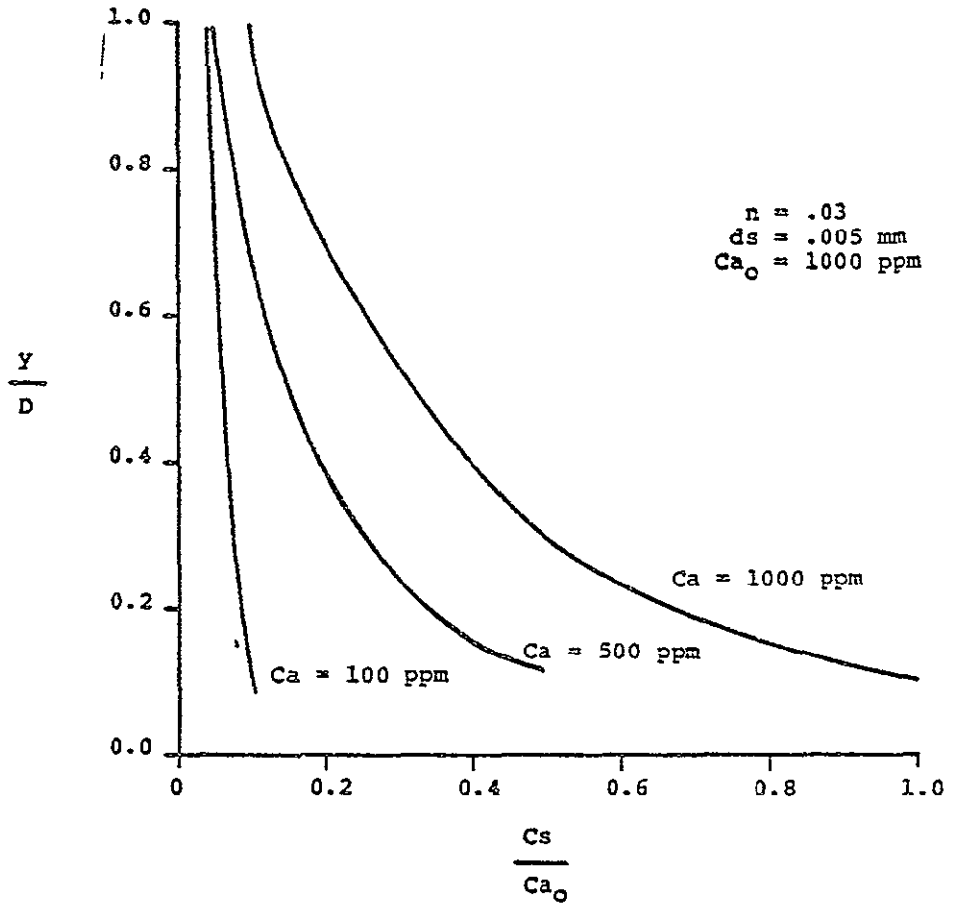

Figure 4.4 Vertical suspended sediment concentration as a function of the reference suspended sediment concentration Ca.

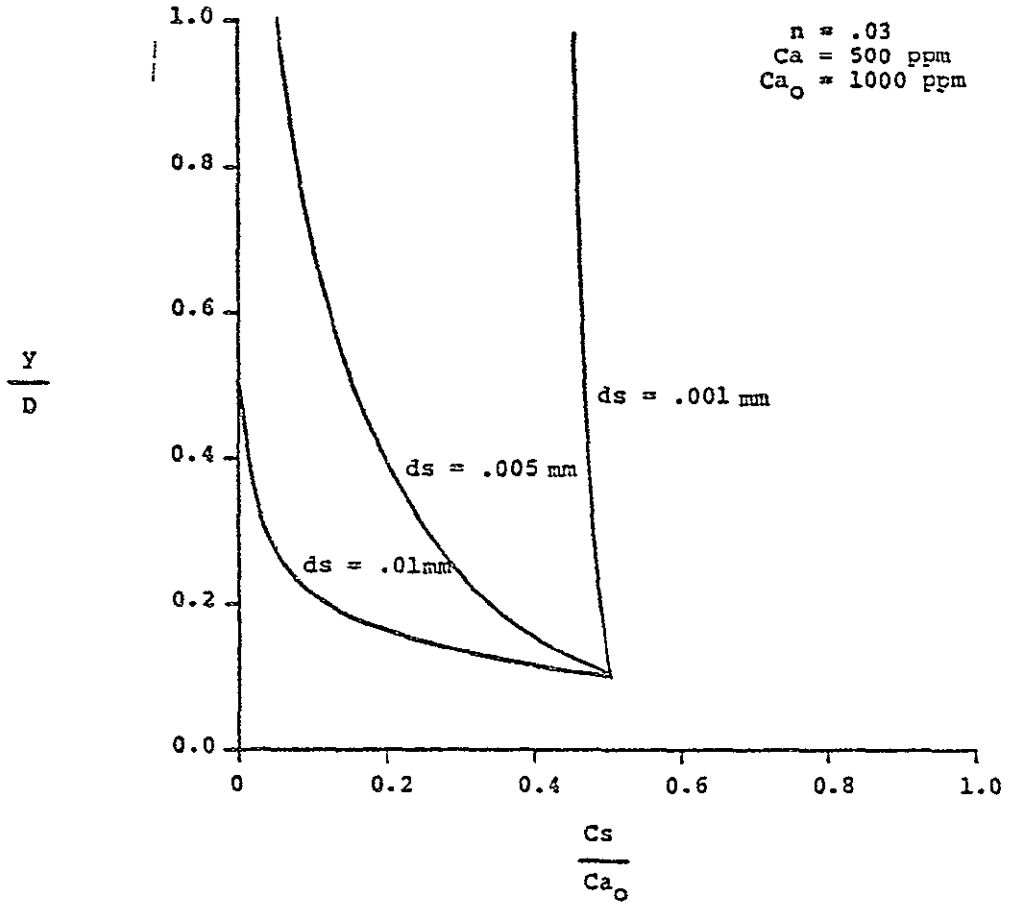

Figure 4.5 Vertical suspended sediment concentration distribution as a function of the mean particle size ds.

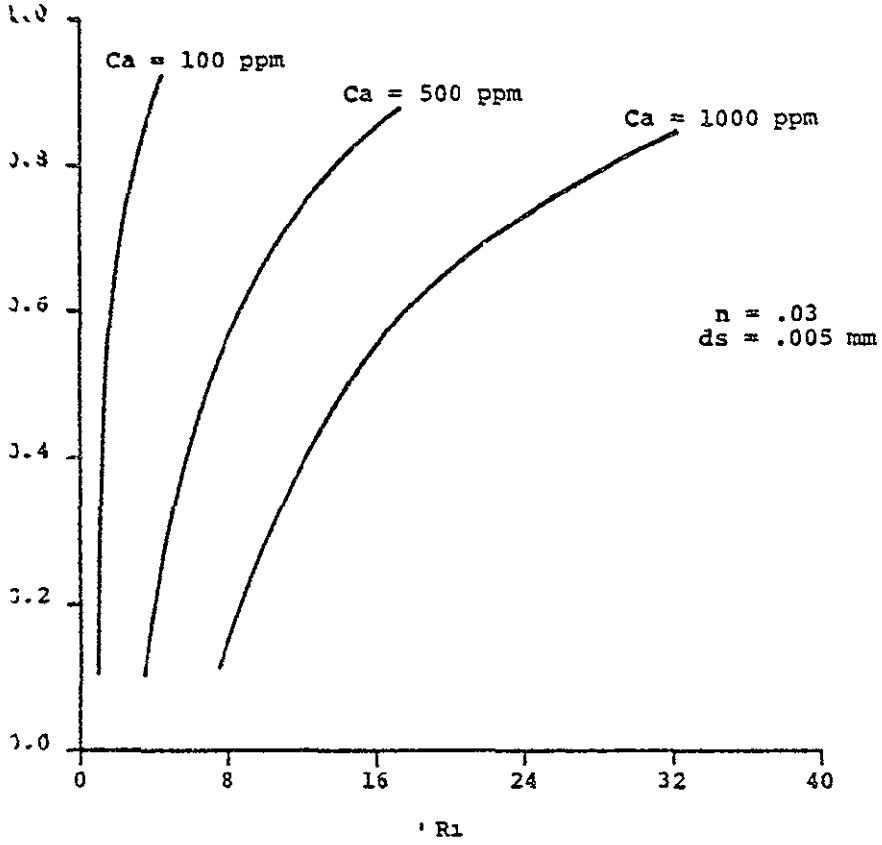

Figure 4.6 Vertical distribution of the Richardson's Number as a function of the reference suspended sediment concentration Ca.

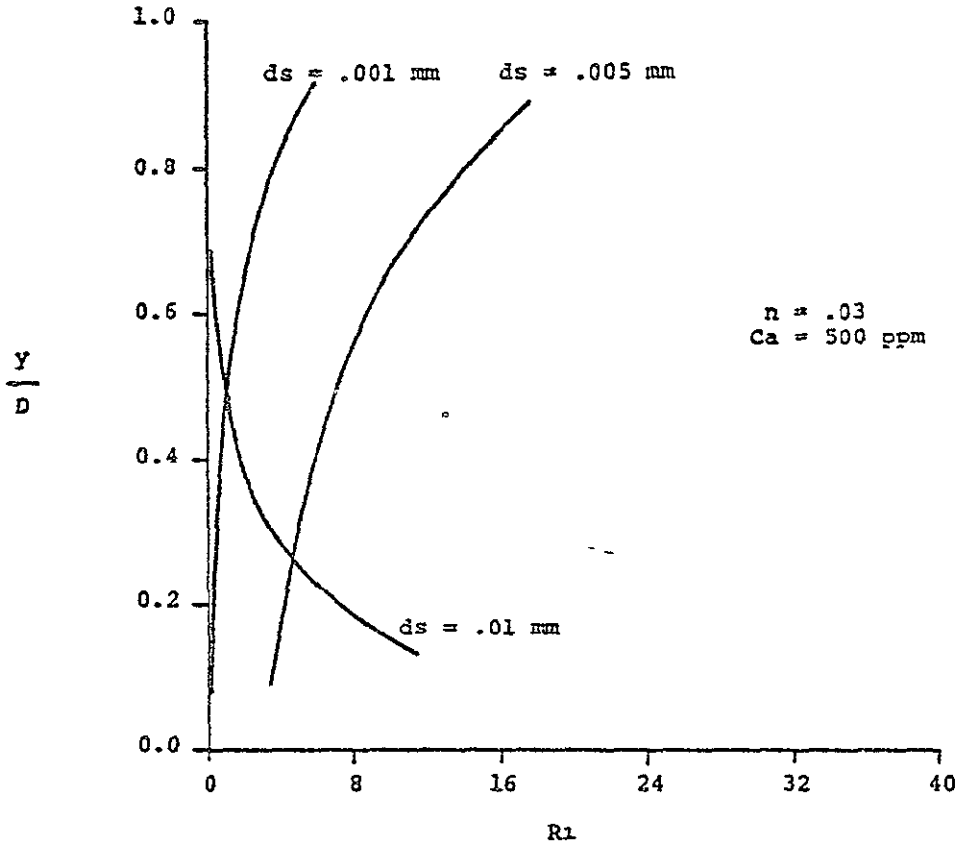

Figure 4.7 Vertical distribution of Richardson's number as a function of the mean particle size ds.

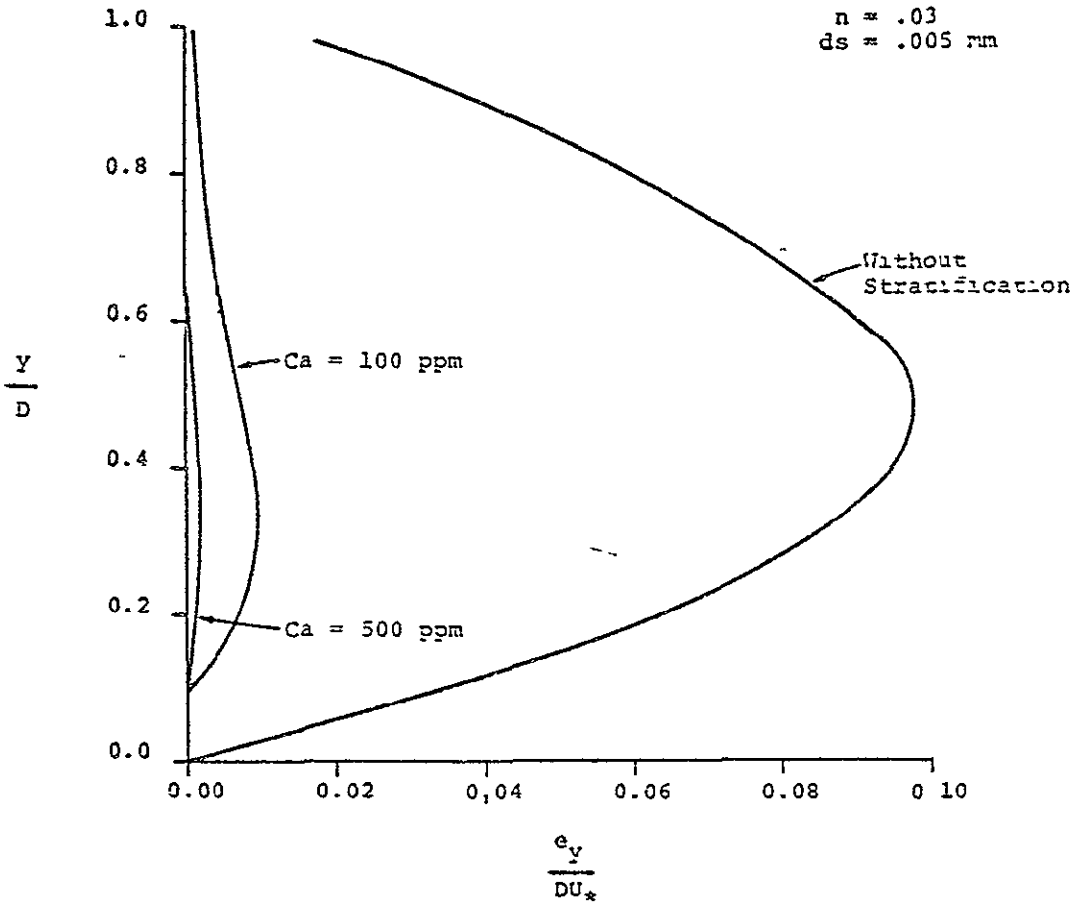

Figure 4 8 Vertical distribution of the turbulent vertical diffusion coefficient as a function of the reference suspended sediment concentration Ca.

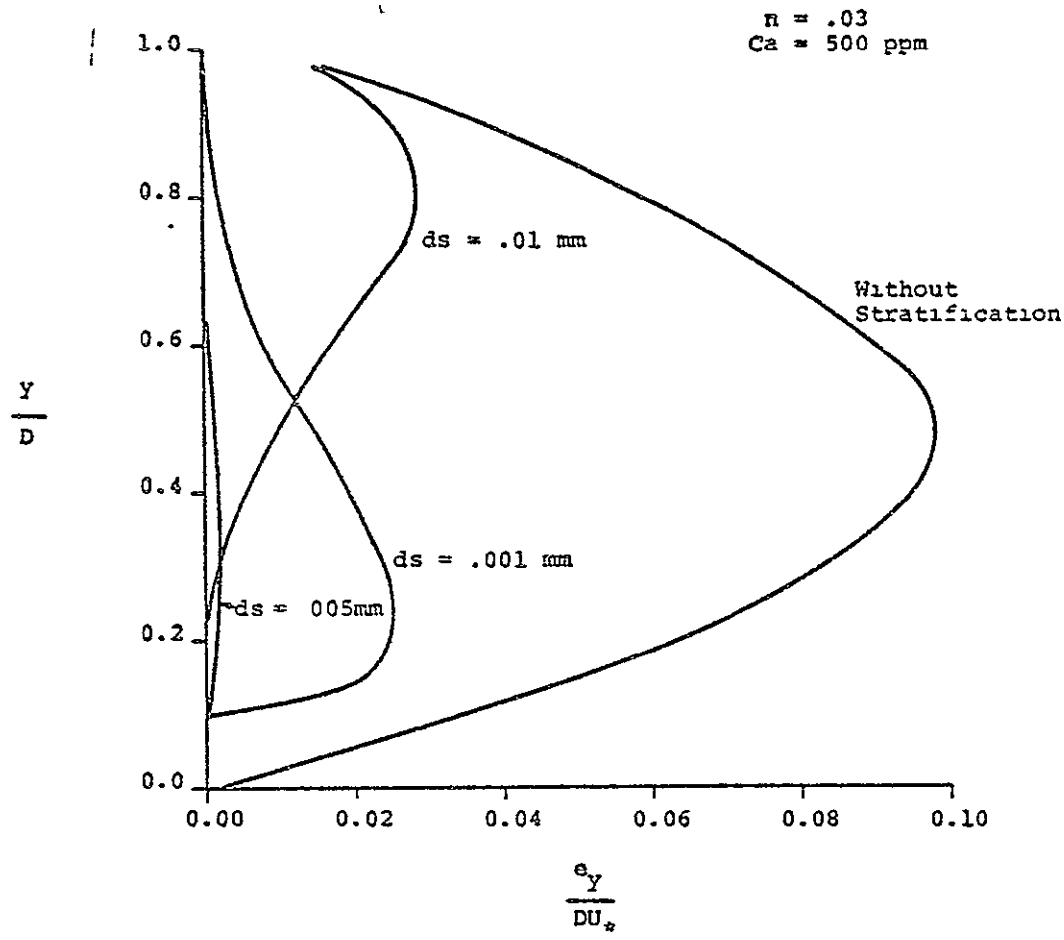

Figure 4.9 Vertical distribution of the turbulent vertical diffusion coefficient as a function of the mean particle size ds

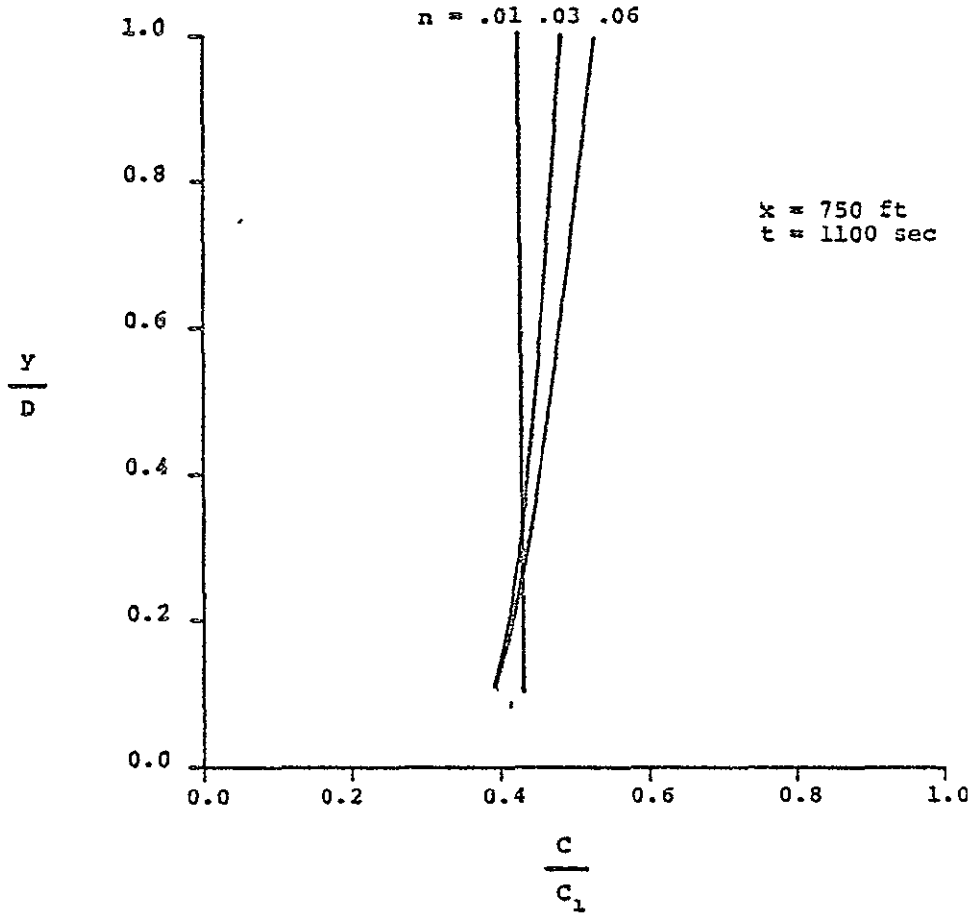

Figure 5.1 Vertical pollutant concentration profile as a function of Manning's roughness coefficient n.

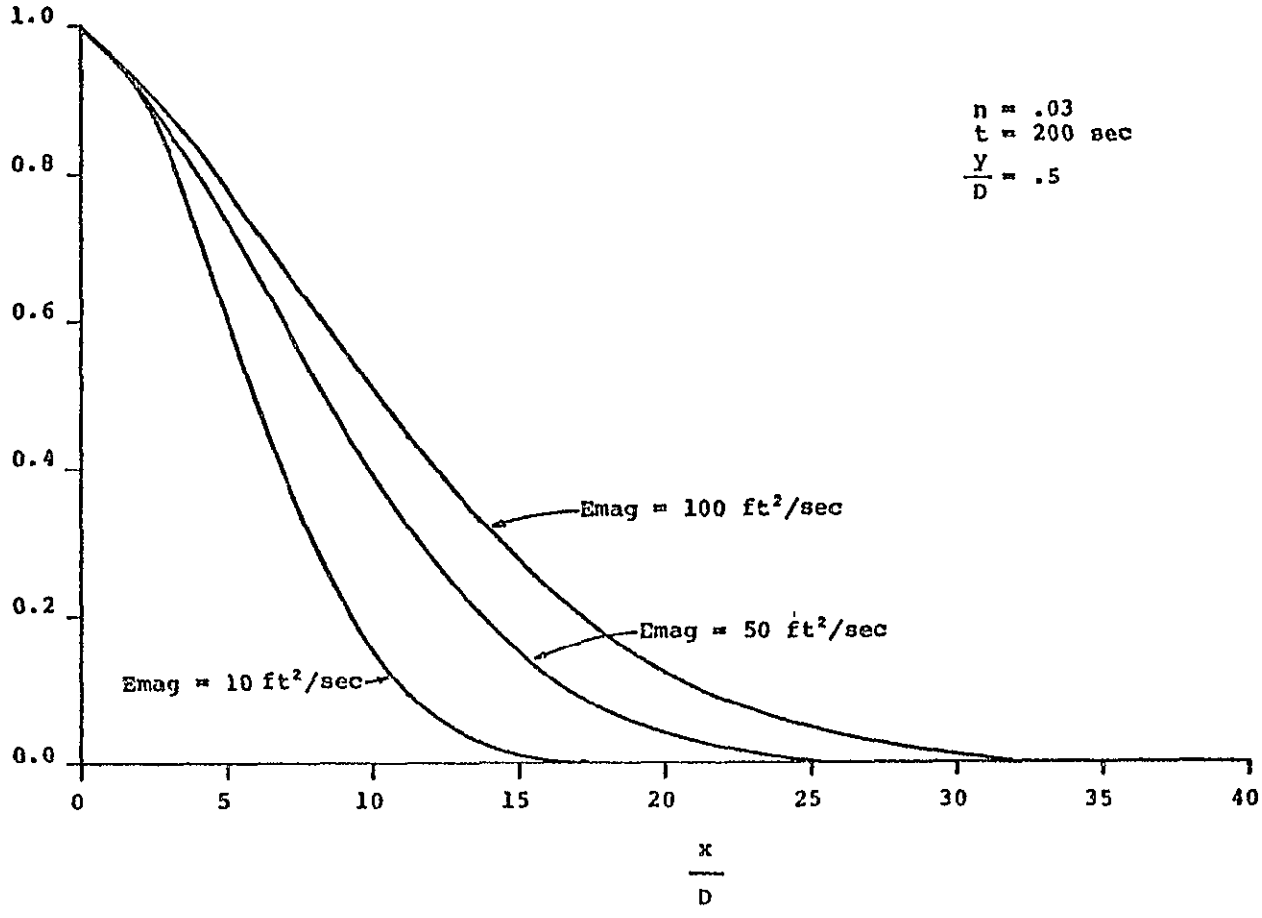

Figure 5.2a Longitudinal pollutant concentration profile as a function of the magnitude of the longitudinal diffusion coefficient.

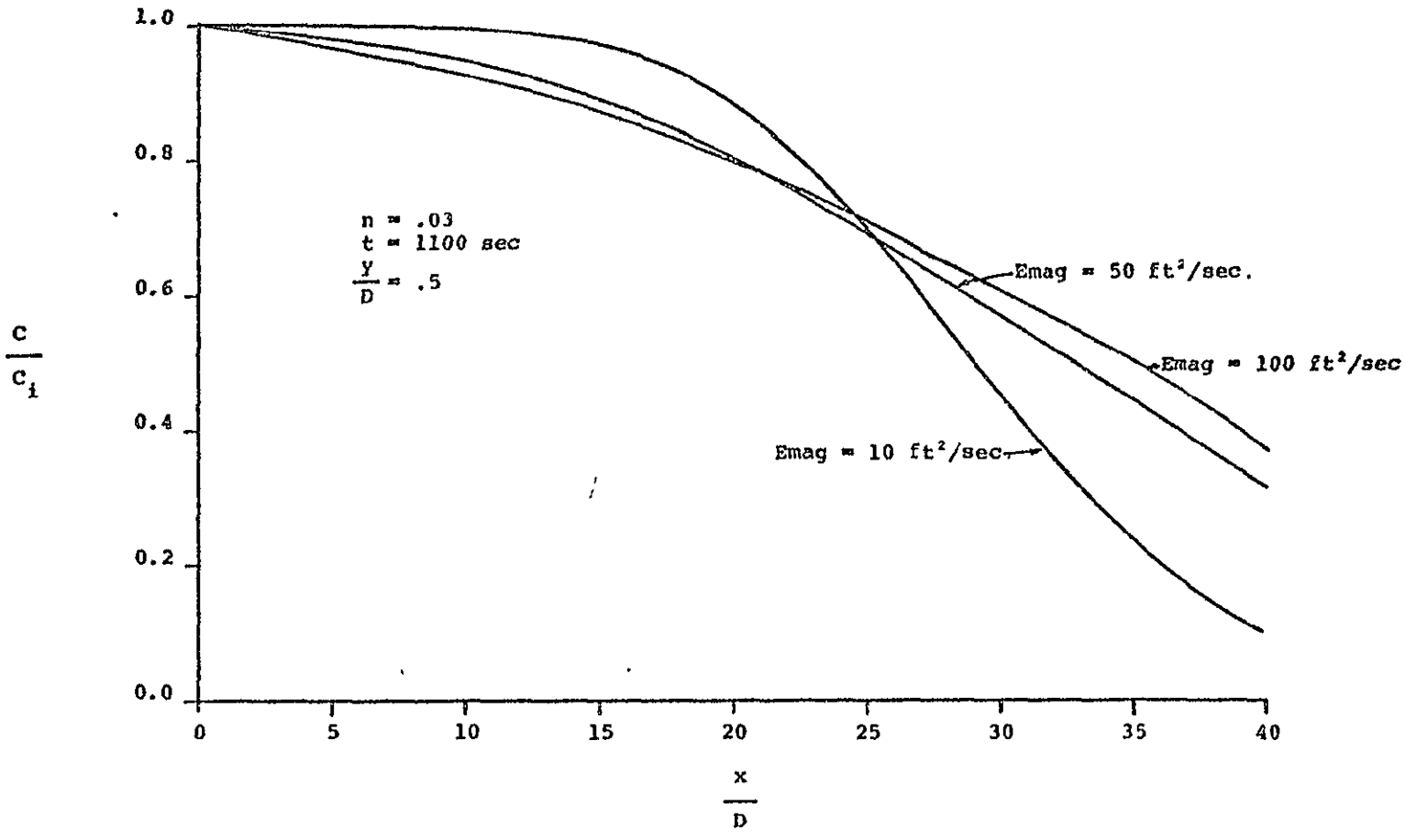

Figure 5.2b Longitudinal pollutant concentration profile as a function of the magnitude of the longitudinal diffusion coefficient

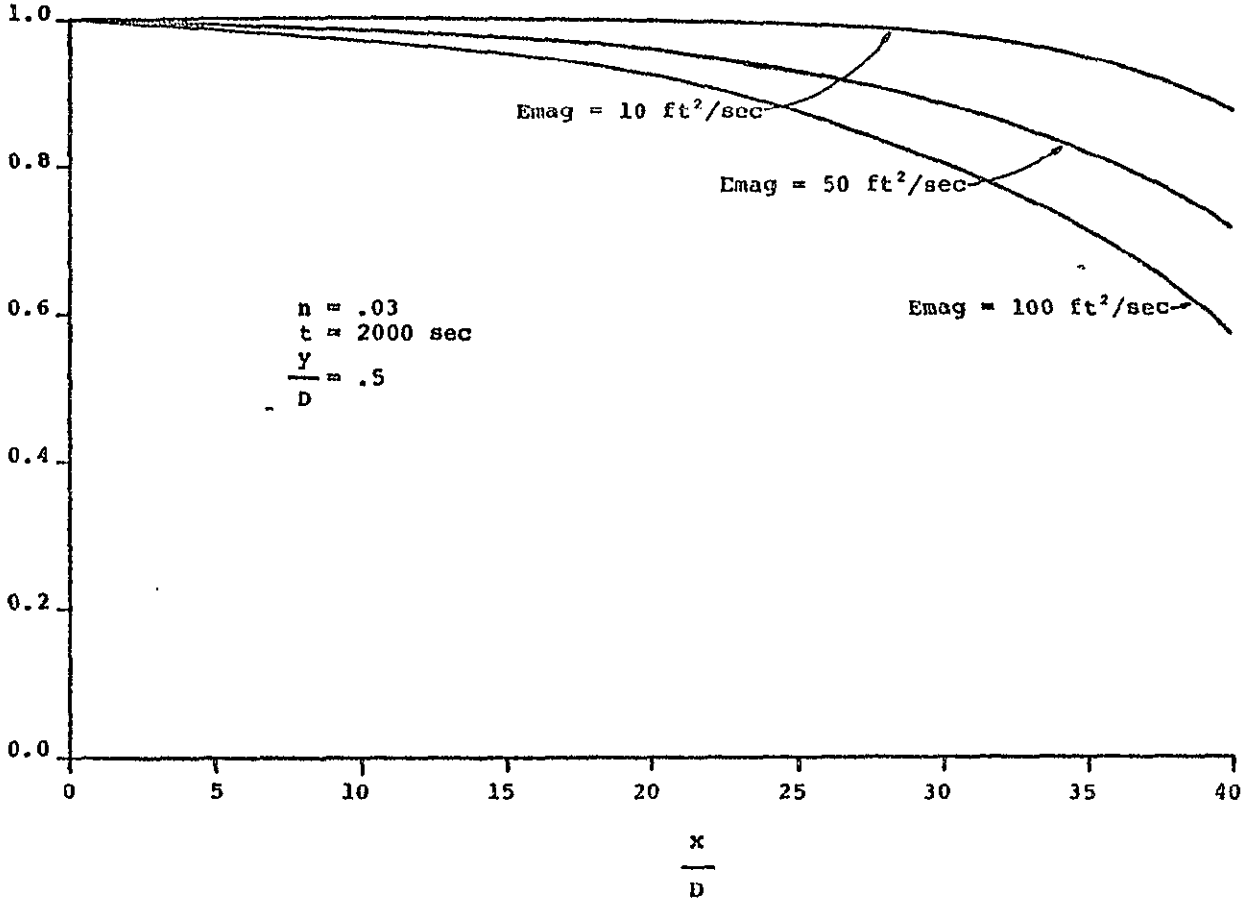

Figure 5.2c Longitudinal pollutant concentration profile as a function of the magnitude of the longitudinal diffusion coefficient

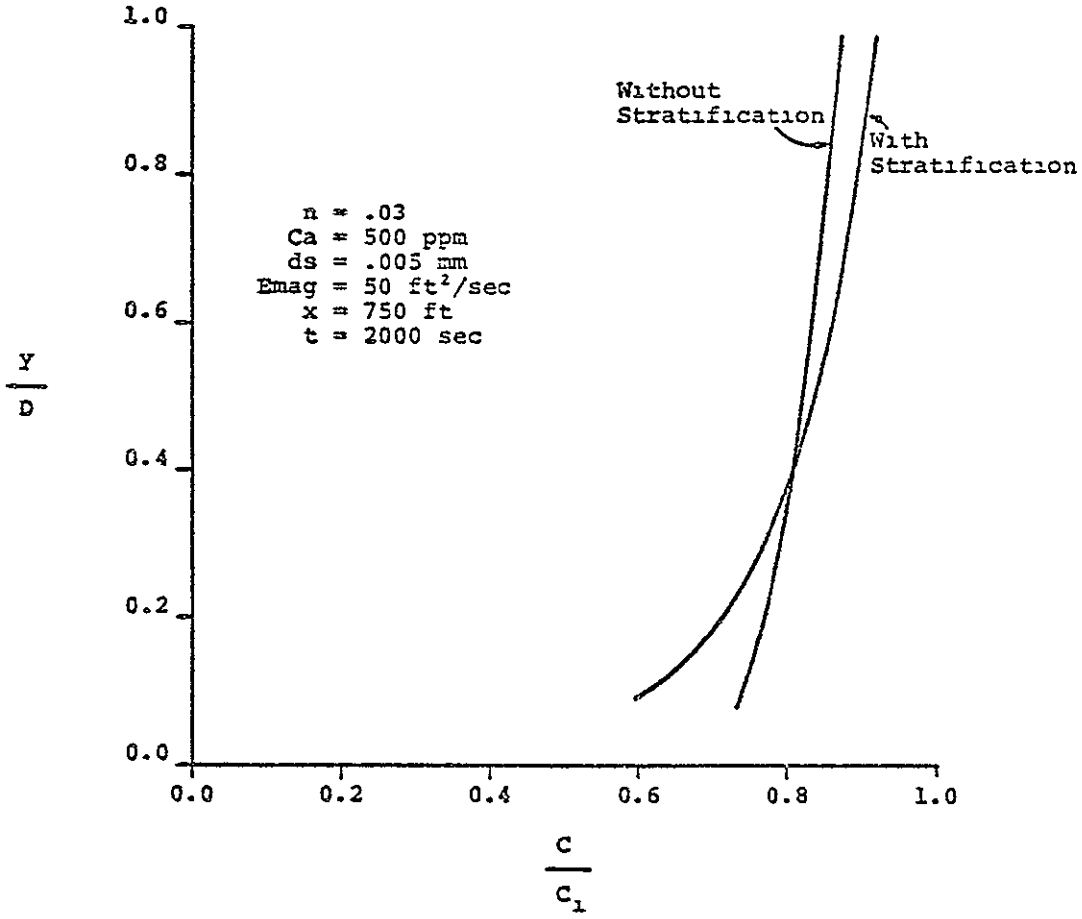

Figure 5.3 Vertical pollutant concentration profiles illustrating the influence of stratification.

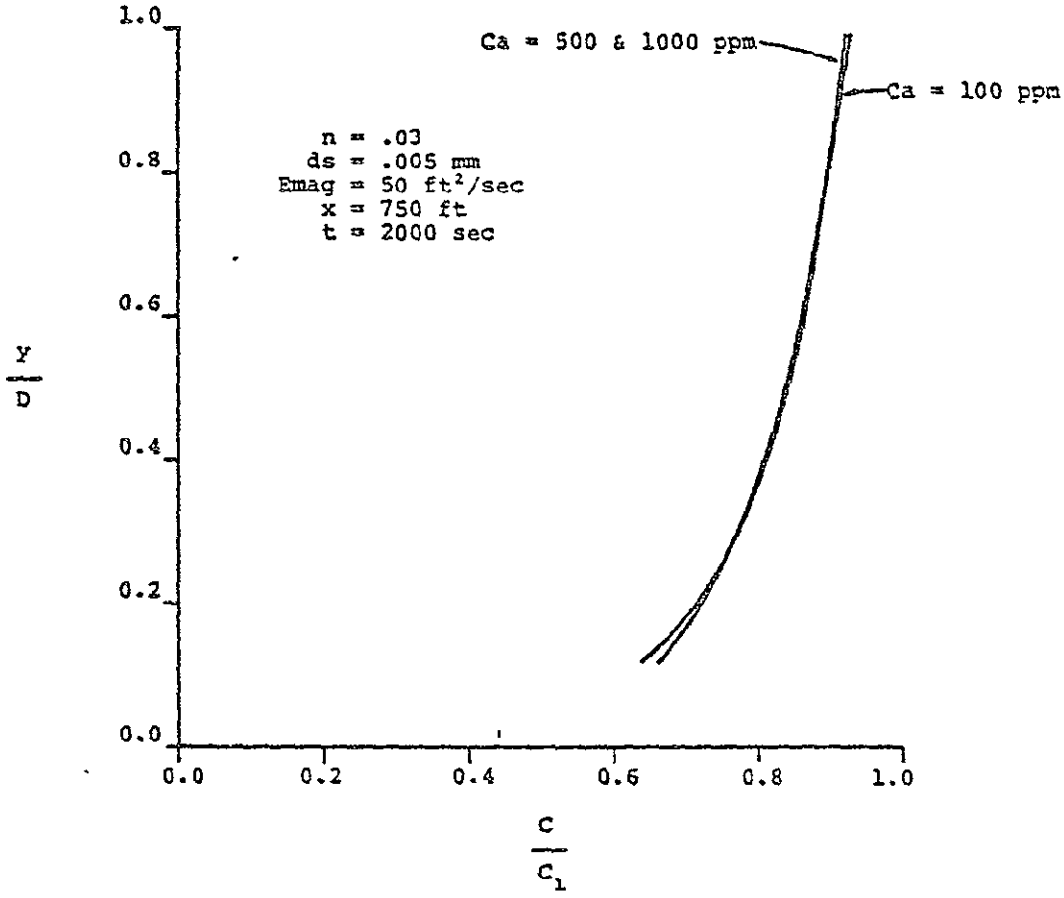

Figure 5.4a Vertical pollutant concentration profiles illustrating the effects of varying suspended sediment concentration on the influence of stratification

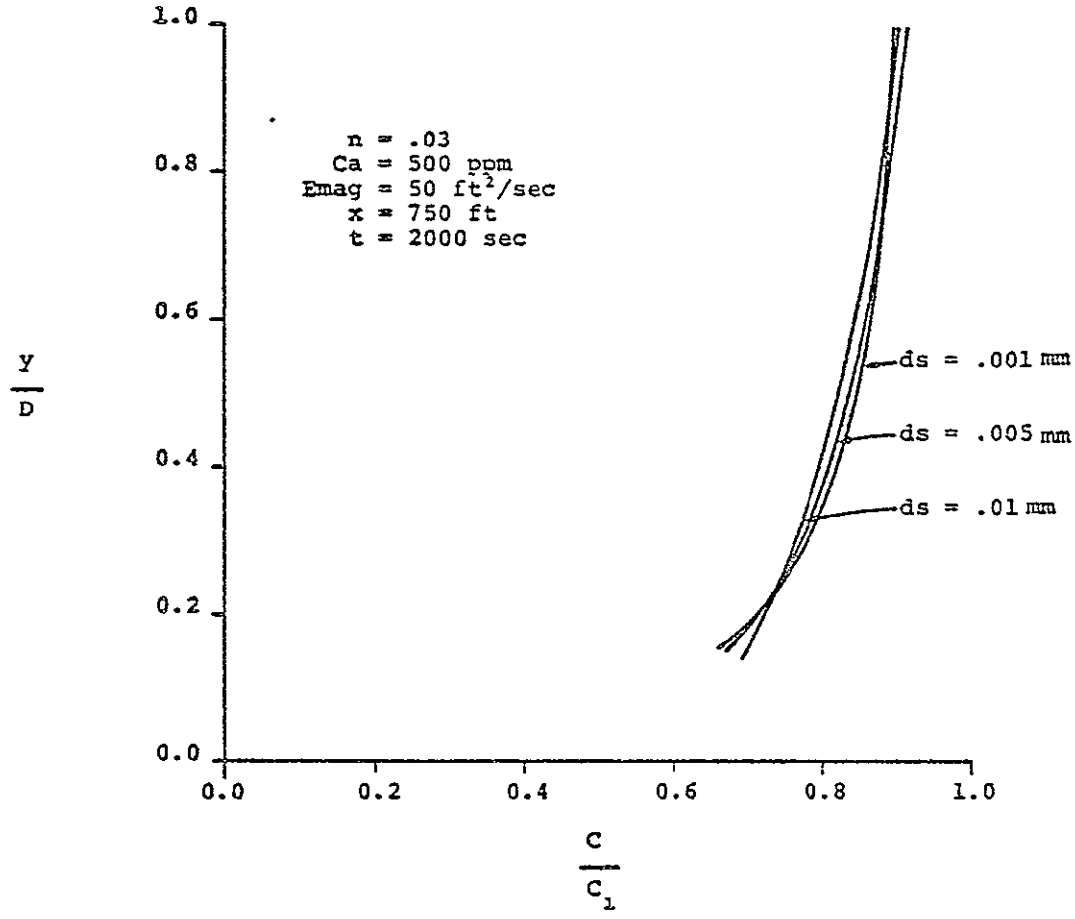

Figure 5.4b Vertical pollutant concentration profiles illustrating the effect of varying mean particles size on the influence of stratification.

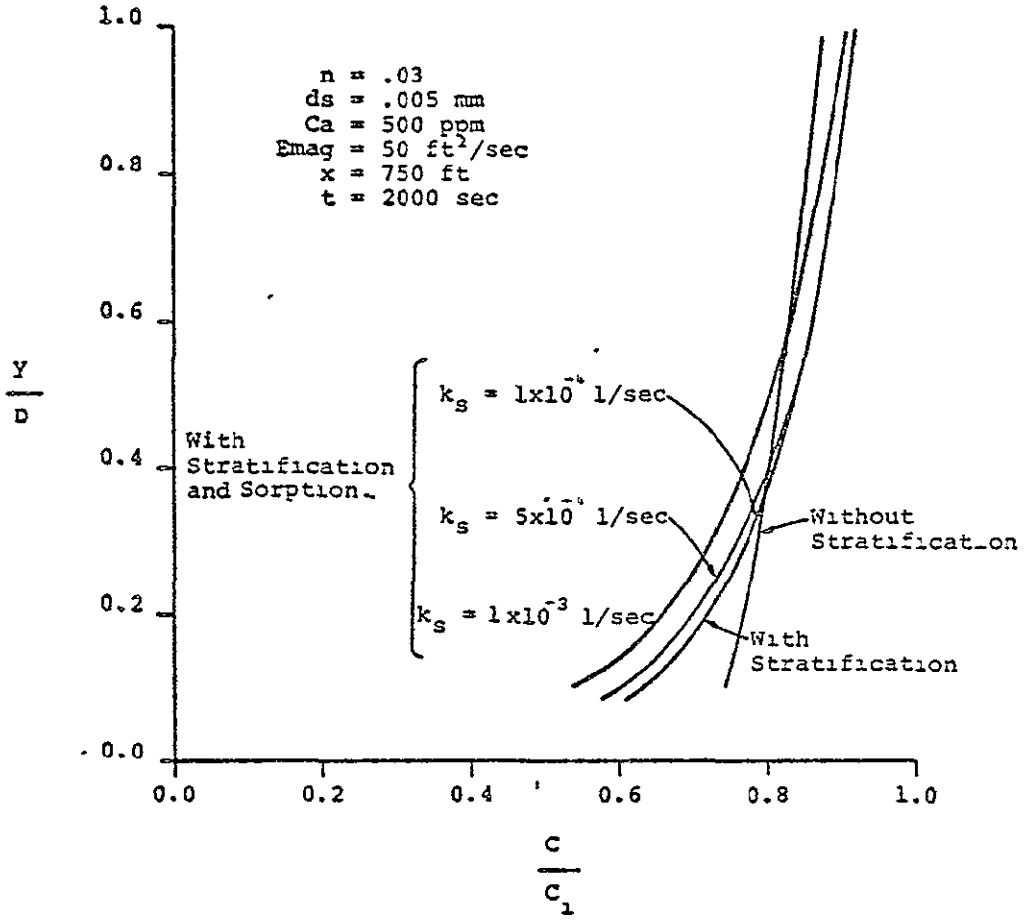

Figure 5.5 Vertical pollutant concentration profiles illustrating the uptake of mercury as a function of the sorption parameter k_s.

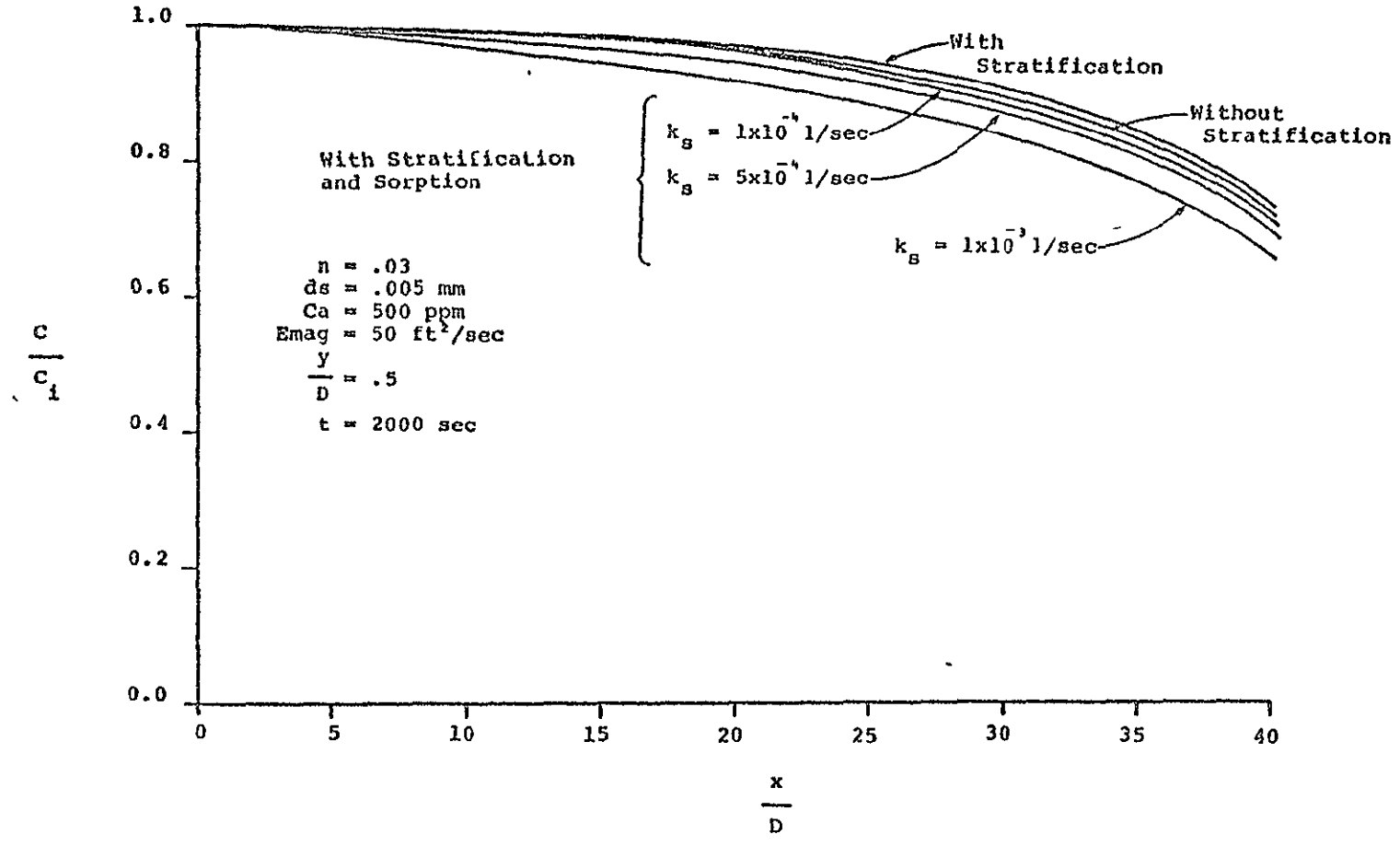

Figure 5.6a Longitudinal pollutant concentration profiles illustrating the uptake of Mercury as a function of the sorption parameter k_S.

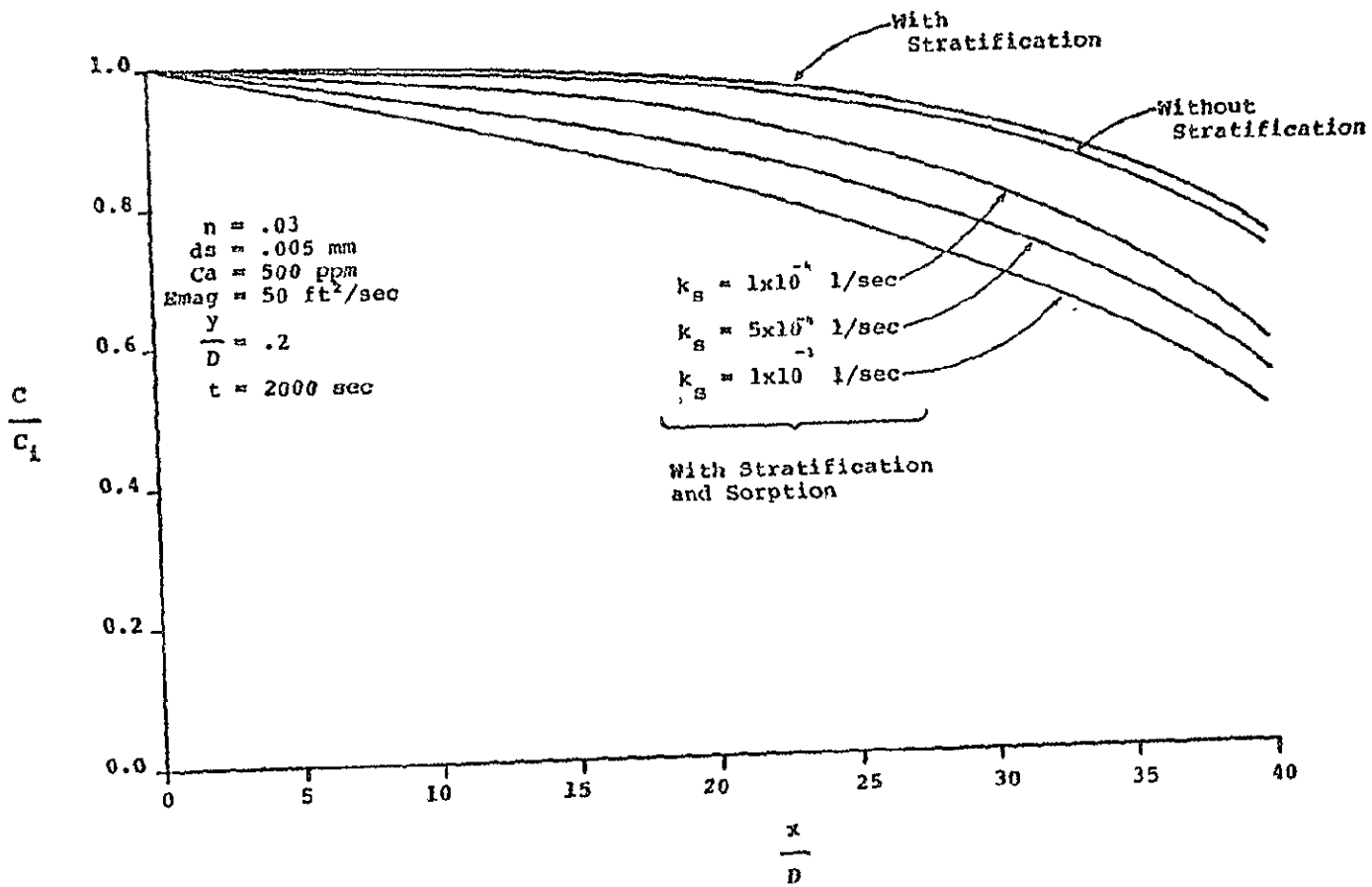

Figure 5.6b Longitudinal pollutant concentration profiles illustrating the uptake of Mercury as a function of the sorption parameter k_s.

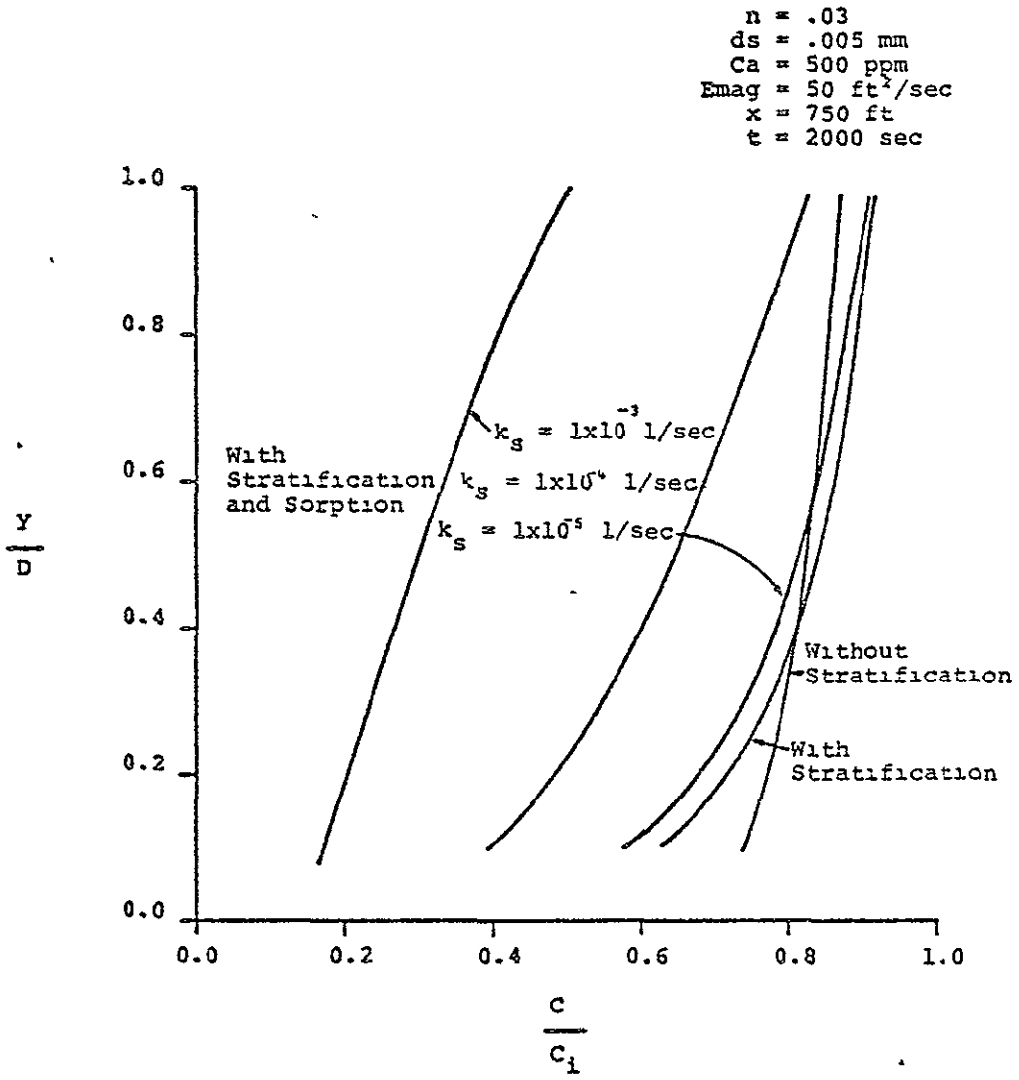

Figure 5.7 Vertical pollutant concentration profiles illustrating the uptake of DDT as a function of the sorption parameter k_s.

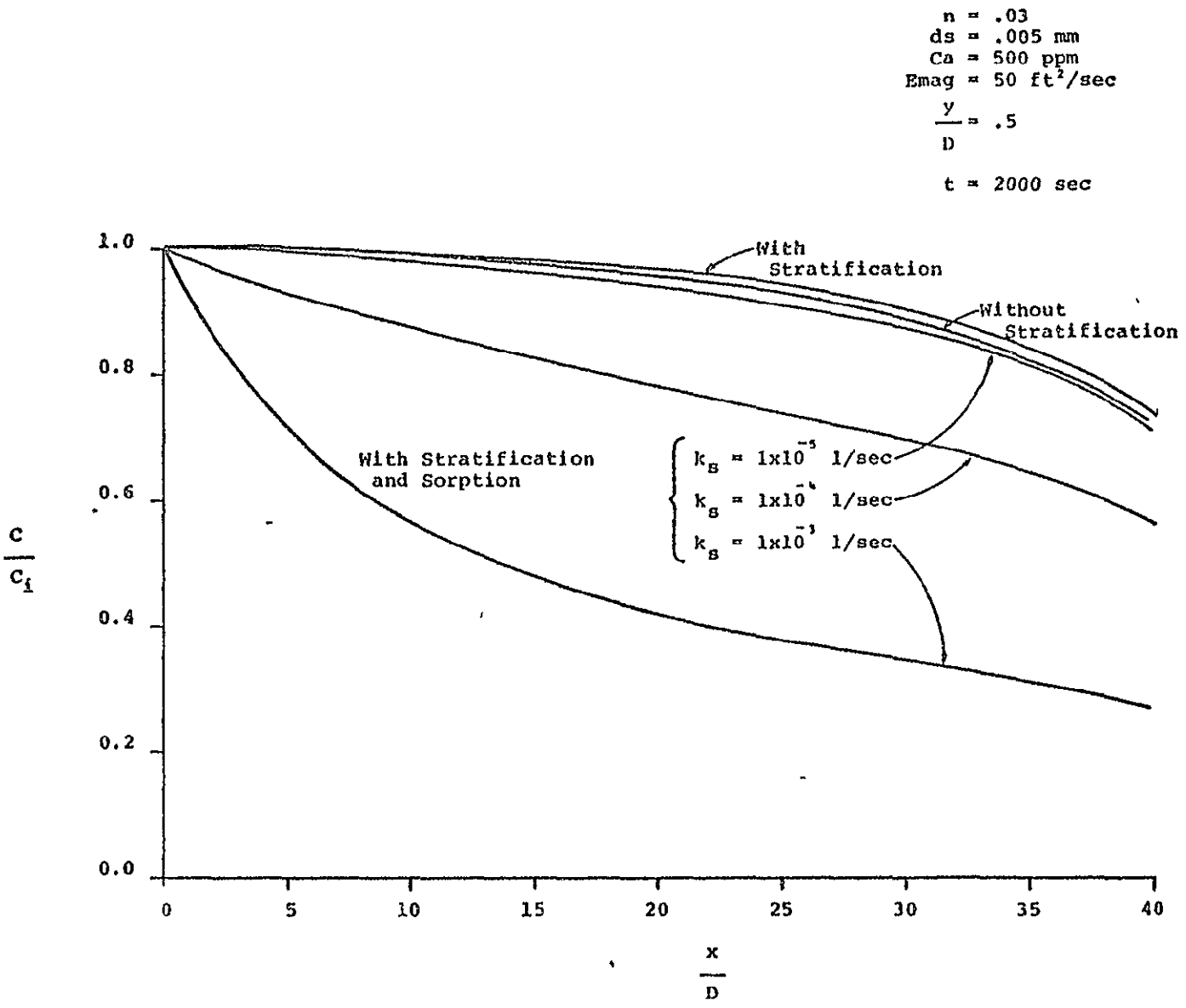

Figure 5.8 Longitudinal pollutant concentration profiles illustrating the uptake of DDT as a function of the sorption parameter ks.

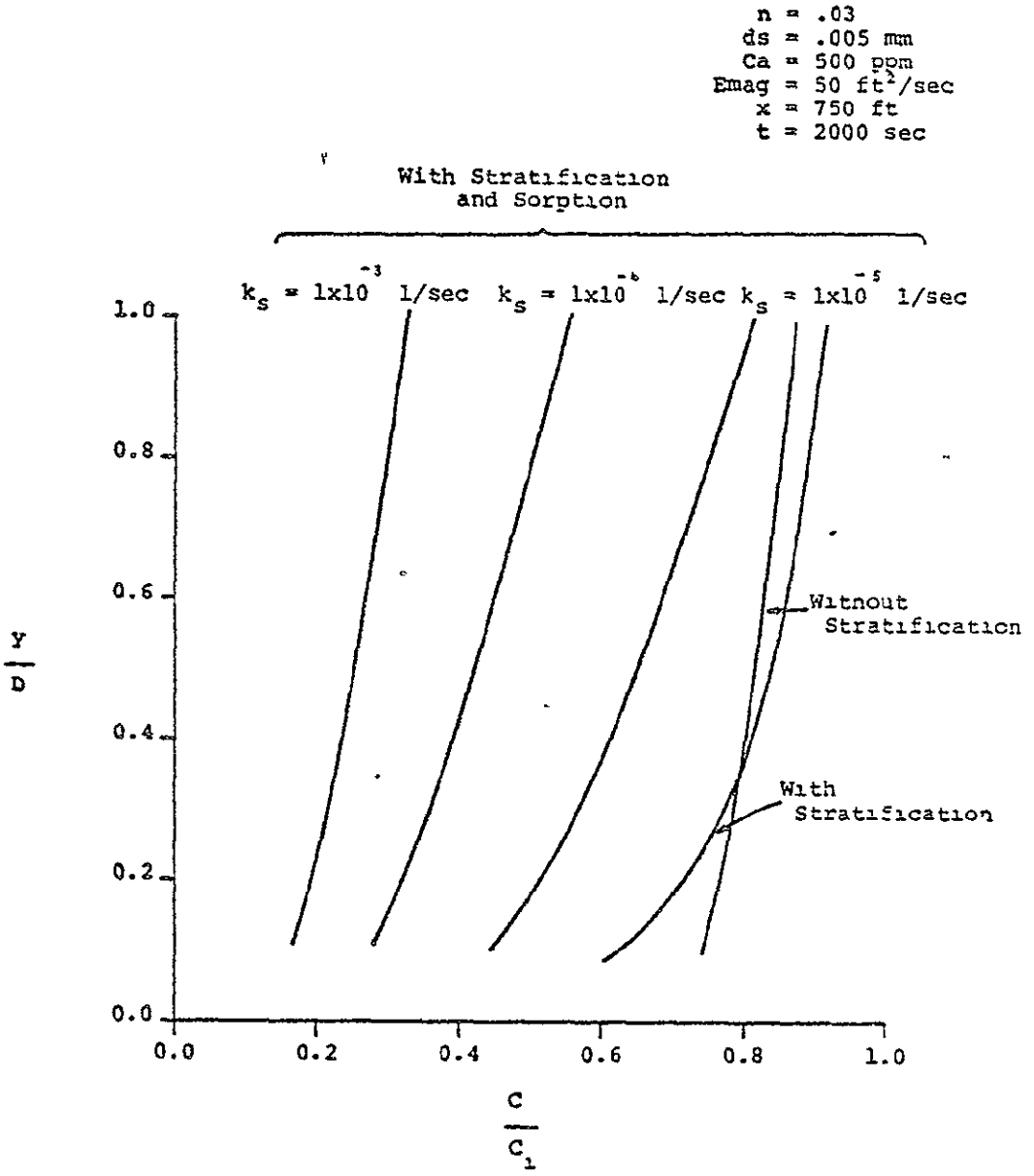

Figure 5.9 Vertical pollutant concentration profiles illustrating the uptake of Heptachlor as a function of the sorption parameter k_s.

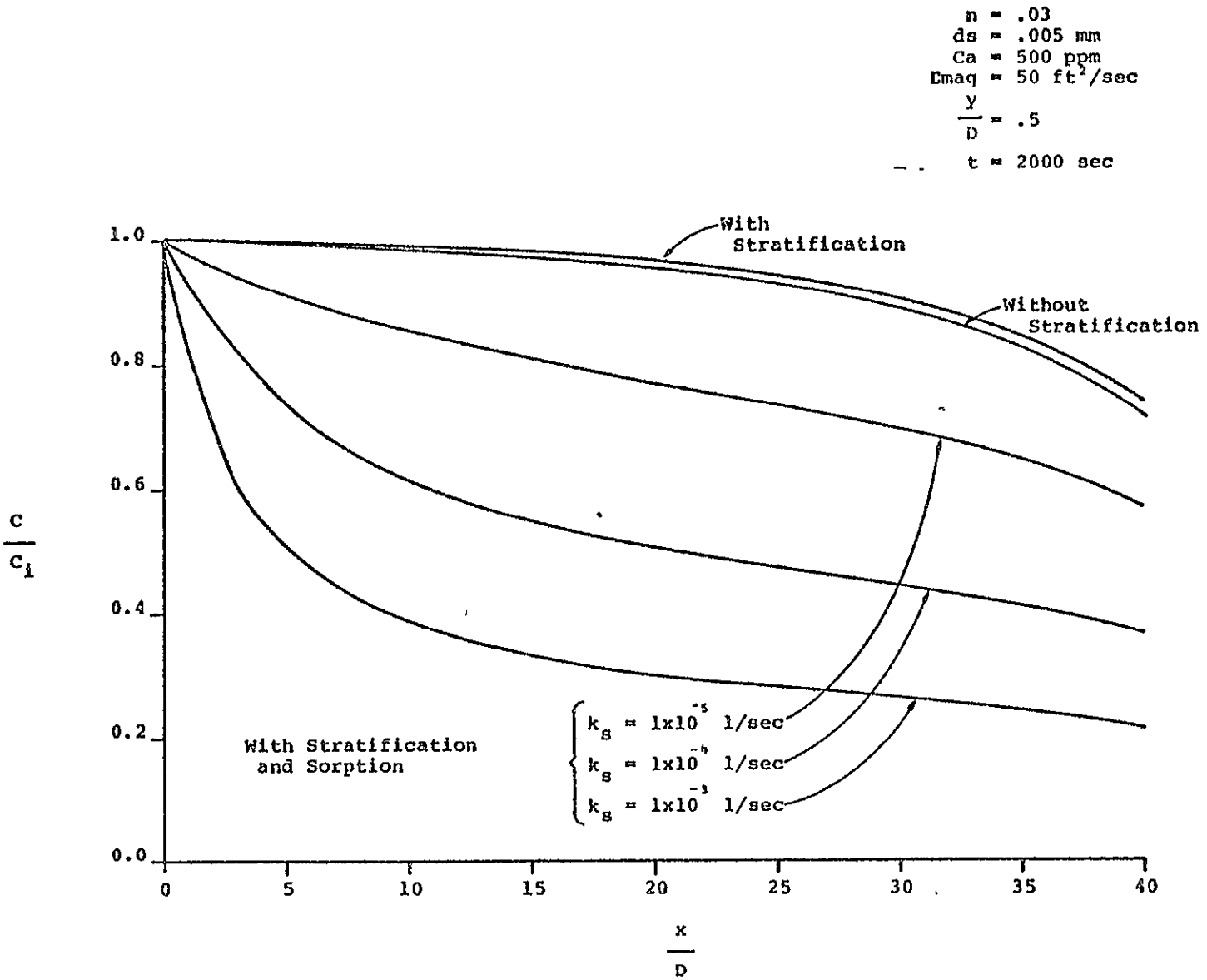

Figure 5.10 Longitudinal pollutant concentration profiles illustrating the uptake of Heptachlor as a function of the sorption parameter k_s.